# A comparison of finite strain viscoelastic models based on the multiplicative decomposition

F. Gouhier, J. Diani

# A comparison of finite strain viscoelastic models based on the multiplicative decomposition

F. Gouhier[a], J. Diani[a]

[a]*Laboratoire de Mécanique des Solides,UMR 7649, École Polytechnique, 91128 Palaiseau, France*

**Abstract**

The constitutive equations of several finite strain viscoelastic models, based on the multiplicative decomposition of the deformation gradient tensor and written in a thermodynamically consistent framework, are reviewed to demonstrate their similarities and differences. The proposed analysis shows that dissipation formulations, which may appear different, are similar when formulated in the same configuration, allowing the definition of a unified *general model*. Then, the *general model*'s ability to reproduce the main features of the behavior of rubbers is explored. First, by comparing its responses to the ones of finite linear viscoelastic models commonly implemented in commercial finite element codes. Cases of monotonic uniaxial tension and simple shear, relaxation, and sinusoidal simple shear are considered. Second, by confronting a classic generalized Maxwell rheological scheme to a Zener one with a non-constant viscosity and exploring the relevance of both options within the *general model*'s constitutive equations.

*Keywords:* Finite strain, Time-dependent, Viscosity, Nonlinear, Dissipation

## 1. Introduction

Rubbers are viscoelastic materials that may undergo very large strain, so they are generally modeled in a finite strain framework. The main features of their time-dependent stress-strain responses have been extensively characterized in monotonic and cyclic tests when varying the strain rate or frequency and modulating the strain amplitude, sometimes including relaxation or creep steps. The experimental results report strong non-linearities, including the Payne effect (Payne, 1962; Rendek and Lion, 2010; Delattre et al., 2016), with strain-dependent softening upon first load

*Email addresses:* florian.gouhier@polytechnique.edu (F. Gouhier), julie.diani@polytechnique.edu (J. Diani)

known as the Mullins effect (Mullins, 1969), hysteretic behavior even at low strain rate (Bergström and Boyce, 1998; Amin et al., 2006; Diani et al., 2006), and stress relaxation depending on the applied strain (Amin et al., 2006). Some of these features are also witnessed in other soft materials, like biological tissues, hydrogels, and propellants, whose constitutive equations very often rely on models initially written for rubbers (Bergström and Boyce, 2001; Haslach, 2005; Samadi-Dooki and Voyiadjis, 2019; Mao et al., 2017; Özüpek and Becker, 1992; Kumar et al., 2018). So far in the literature, two prevalent approaches have been used to describe the dissipative processes arising in finite strain viscoelasticity for these materials: the hereditary integrals and the internal state variable formulation with differential evolution equations.

The former relies on an extension of the Boltzmann superposition principle to the finite strain theory, resulting in a relationship between the stress tensor and the total strain history through a nonlinear constitutive functional. The first constitutive model introducing such a strain memory is to the credit of Green and Rivlin (1959), where the stress response is described by means of multiple integral constitutive equations, also known as the Volterra integral series. Based on the fading memory assumption, Coleman and Noll (1960, 1961) introduced a theory not limited to infinitesimal strain but restricted to the recent past, then extended by (Wang, 1965). Pipkin and Rogers (1968) approximated the multi-step strain history by a linear combination of single step strain functions through a nonlinear hereditary integral, this framework encompassing all formerly developed theories. As for other noteworthy models using this approach (Bernstein et al., 1963; Lockett, 1972; Christensen, 1980; Fung, 1981), only a single hereditary integral including different constitutive assumptions is generally held for numerical purposes and to ease the material parameter identification. The main problem of this approach stands in the fact that strong nonlinearities with large perturbations from the thermodynamic equilibrium would require high-order multiple nonlinear integrals from the Volterra developments. For further details on the hereditary integral approach, the reader may refer, for instance, to (Drapaca et al., 2007; Wineman, 2009).

In a first effort to use the internal state variable framework, Schapery (1964, 1966) described the stress-strain relationship with nonlinear elastic and linear viscoelastic constitutive equations, also called "finite linear viscoelasticity", for which the internal variable was of non-equilibrium stress or overstress nature. One of the first implementations of this kind is from Simo (1987), who introduced an additive split of the stress into equilibrium and non-equilibrium parts, as well as a linear rate equation for internal stress variables, to define a viscoelastic model. This framework has been taken over (Simo and Ju, 1989; Özüpek and Becker, 1992; Holzapfel and

Simo, 1996; Kaliske and Rothert, 1997; Holzapfel et al., 2002), mainly due to its computational efficiency (Govindjee and Simo, 1992). It remains the default model in large strain viscoelasticity for several finite element software, such as Abaqus, Ansys, Comsol, or Nastran. However, due to the linear evolution law, the model is designed for small perturbations from the equilibrium state (Reese and Govindjee, 1997; Haslach, 2005; Latorre and Montáns, 2016). Furthermore, it has been shown to produce some unphysical responses (Yagimli et al., 2023), and its thermodynamic consistency remains a topic of debate even recently (Govindjee et al., 2014; Liu et al., 2021).

Another path has been to consider viscoelastic strain internal variables. Extending the work of Green and Tobolsky (1946), Lubliner (1985) applied the multiplicative decomposition of the deformation gradient tensor from (Sidoroff, 1974) to propose a linear evolution equation for its strain internal variables. The case of finite linear viscoelasticity was finally overcome with two finite strain viscoelastic models (Le Tallec et al., 1993; Lion, 1997), both based on the same multiplicative decomposition and validating the second law of thermodynamics. However, Le Tallec et al. (1993) considered incompressible materials only and implemented the simpler finite linear viscoelasticity version of their model, and Lion (1997) did not propose a numerical implementation. As a result, Reese and Govindjee (1998) proposed the most complete version of such a finite nonlinear viscoelastic model for compressible materials, including a finite element code implementation.

These three models, written on the same basis, use different strain internal variables to characterize the viscoelasticity and different evolution laws, according to the modeling configuration, either reference (Le Tallec et al., 1993), intermediate (Lion, 1997) or current (Reese and Govindjee, 1998). Later, other finite viscoelastic models using strain energy densities based on the Zener or generalized Maxwell schemes (for instance (Huber and Tsakmakis, 2000; Amin et al., 2002; Kumar and Lopez-Pamies, 2016)) have been written with either of the evolution laws proposed by the three pioneering contributions. One may note that the Poynting-Thomson rheological scheme has rallied less interest, albeit constitutive equations written in the intermediate configuration (Huber and Tsakmakis, 2000) or the reference one exist (Boukamel et al., 2001; Méo et al., 2002; Laiarinandrasana et al., 2003).

To better represent the highly nonlinear viscoelastic stress-strain responses of rubbers, Bergström and Boyce (1998) considered a Zener model with a non-constant viscosity, on top of adding some physical meaning to their constitutive equations. This option was also adopted by other authors, in the case of a generalized Maxwell model with viscosities depending on the strain amplitude (Rendek and Lion, 2010; Delattre et al., 2016) to reproduce the Payne effect, or in the case of a Zener model to

avoid dealing with multiple viscoelastic branches, as reviewed in (Ricker et al., 2023). The model (Kumar and Lopez-Pamies, 2016), which provides the best representations of the cyclic uniaxial tension behavior of rubbers, defines the viscosity as dependent on six parameters and two coupled internal variables. Until now, to the author's knowledge, it has not been shown how the viscosity evolved during simple tests, such as cyclic uniaxial tension or cyclic simple shear. By doing so, we aim to compare the responses of this model to those of a classic generalized Maxwell model with constant parameters for simple loading cases. The purpose is thus to highlight the advantages and limitations of the defined viscosity function.

Therefore, the classic finite strain viscoelastic framework is recalled in what follows, as well as the chosen main constitutive assumptions and their consequences. Then, a review of three models (Le Tallec et al., 1993; Lion, 1997; Reese and Govindjee, 1998) is proposed, highlighting their main differences and similarities by rewriting them with the same quantities and unified notations. Based on the results, a comparative study of the finite linear viscoelastic model of Simo (1987) with the finite viscoelastic evolution equations is proposed through classic loadings exhibiting time-dependent behavior. Lastly, characteristic features displayed by Zener models with non-constant viscosities, as well as the Prony series, are shown through different tests to provide future users with a clearer vision of their choices.

## 2. General constitutive equations

The classic variables within the finite viscoelastic framework, along with useful tensor notations and mathematical operations, are listed in A.5 from Appendix A.

### *2.1. Kinematics*

Considering $\boldsymbol{\chi}$ the mapping function between positions of a material point $M$, $\mathbf{X}(M)$ in the reference configuration $\mathcal{C}_0$ and $\mathbf{x}(M)$ in the current configuration $\mathcal{C}_t$, the material deformation gradient writes as $\mathbf{F} = \nabla_{\mathbf{X}} \boldsymbol{\chi}(\mathbf{X}, t)$, and allows transforming any vector $d\mathbf{X}$ from $\mathcal{C}_0$ into $d\mathbf{x} = \mathbf{F} d\mathbf{X}$ in $\mathcal{C}_t$. The transformation Jacobian, $J = \det(\mathbf{F})$, characterizes the material volume change, while the polar decomposition,

$$\mathbf{F} = \mathbf{R}\,\mathbf{U} = \mathbf{V}\,\mathbf{R}, \tag{1}$$

defines the symmetric positive definite right and left pure stretch tensors, $\mathbf{U}$ and $\mathbf{V}$, and the orthogonal tensor $\mathbf{R}$ associated with pure rotation motions.
The symmetric right and left Cauchy-Green tensors, $\mathbf{C}$ and $\mathbf{b}$, are introduced as,

$$\mathbf{C} = \mathbf{F}^T\,\mathbf{F} = \mathbf{U}^2\,, \qquad \mathbf{b} = \mathbf{F}\,\mathbf{F}^T = \mathbf{V}^2, \tag{2}$$

operating on the reference and current configurations respectively, and associated strain measures are given by the Green-Lagrange $\mathbf{E}$ and Euler-Almansi $\mathbf{e}$ tensors,

$$\mathbf{E} = \frac{1}{2}\left(\mathbf{C} - \mathbf{I}\right), \qquad \mathbf{e} = \frac{1}{2}\left(\mathbf{I} - \mathbf{b}^{-1}\right). \tag{3}$$

Note that the spatial tensor $\mathbf{e}$ can be retrieved by applying a push-forward of the material strain tensor to the current configuration, $\mathbf{e} = \mathbf{F}^{-T}\,\mathbf{E}\,\mathbf{F}^{-1}$.

**Remark 1.** *At this point, it is worth noting that material or Lagrangian quantities refer to the reference configuration, while spatial or Eulerian ones refer to the current configuration. The push-forward operation transforms a tensor from the reference configuration into its counterpart in the current configuration, while the pull-back is the inverse operation. According to the covariant or contravariant nature of the tensor, the mathematical operation differs, as one will read in what follows. Moreover, push-forward or pull-back operations may be applied between an intermediate configuration and the reference or the current one.*

Denoting $\dot{\mathbf{F}} = \mathbf{l}\,\mathbf{F}$ the material time derivative of the deformation gradient tensor, the spatial velocity gradient tensor is then introduced as $\mathbf{l} = \nabla_{\mathbf{x}}\dot{\mathbf{x}}$. Its additive decomposition into symmetric and skew parts,

$$\mathbf{l} = \mathbf{d} + \mathbf{w}, \tag{4}$$

defines $\mathbf{d} = \frac{1}{2}\left(\mathbf{l} + \mathbf{l}^T\right)$ the rate of deformation and $\mathbf{w} = \frac{1}{2}\left(\mathbf{l} - \mathbf{l}^T\right)$ the spin tensor. Noteworthy point, the following relationship,

$$\dot{\mathbf{C}} = 2\mathbf{F}^T\,\mathbf{d}\,\mathbf{F}, \tag{5}$$

between the right Cauchy-Green tensor rate and the rate of deformation will be useful later.

*2.2. Multiplicative decomposition*

Rubberlike materials may undergo large strain and show nearly incompressible time-dependent behavior leading to multiplicative splits of the deformation gradient tensor into volumetric and isochoric parts (Flory, 1961; Ogden, 1976) on the one hand,

$$\mathbf{F} = J^{1/3}\,\bar{\mathbf{F}}, \tag{6}$$

and into elastic and viscous parts (Sidoroff, 1974) to model rheological Maxwell elements on the other hand,

$$\mathbf{F} = \mathbf{F}_e\,\mathbf{F}_v. \tag{7}$$

**Remark 2.** *Since the introduction of the multiplicative decomposition in elastoplasticity by Lee (1969) and its application to viscoelasticity by Sidoroff (1974), the order in which the decomposition should be performed has been an ongoing debate. In elastoplasticity, the reversed decomposition seems to be kinematically equivalent to Sidoroff's decomposition for isotropic materials (Clifton, 1972; Lubarda, 1999). However, it is worth noting that their physical meanings differ, and the case at hand will define the most suitable decomposition. In the context of viscoelasticity, Latorre and Montáns (Latorre and Montáns, 2015, 2016) proposed a way to model anisotropic finite strain viscoelasticity, using either the Sidoroff decomposition or the reverse decomposition. Interestingly, the nonlinear evolution equations written in a Lagrangian framework are similar for both models (refer to Eq. (68) in (Latorre and Montáns, 2015) and Eq. (40) in (Latorre and Montáns, 2016)). However, only the reverse decomposition allows all defined quantities to be entirely determined in the reference configuration. Furthermore, both models provide different responses even under isotropic conditions when large strain rotational loadings are considered, such as a simple shear test (refer to Figure 5 in Latorre and Montáns (2016)). The debate around viscoelastic materials continues, with Bahreman et al. (2022) recently showing that Sidoroff's decomposition leads to unexpected viscoelastic behavior. However, Sadik and Yavari (2024) argued that the previous observation was based on incorrect assumptions. Additionally, they expected both decompositions to result in an equivalent theory, similar to the decompositions in anelasticity (Yavari and Sozio, 2023). At this point, Sidoroff's decomposition seems preferable in the case of isotropic viscosity, while the reversed one appears more interesting in the anisotropic case.*

Doing so introduces an intermediate configuration corresponding to the fictive unrelaxed state obtained after the instantaneous removal of the elastic deformation gradient (Figure 1). Contrary to elastoplasticity, note that the intermediate configuration in viscoelasticity is generally not stress free (Latorre and Montáns, 2016; Sadik and Yavari, 2024).

**Remark 3.** *The nature of the intermediate configuration introduced to model viscoelasticity has often led to confusion. Given that the viscoelastic multiplicative decomposition originated from elastoplasticity, these two kinds of modeling were frequently mistakenly considered as similar dissipative processes, even though they are very different in nature. Recently, Sadik and Yavari (2024) addressed this issue by comparing the stress in the intermediate state in viscoelasticity and anelasticity (e.g., elastoplasticity). While the stress completely vanishes in the latter case, it is shown that the intermediate configuration in viscoelasticity is generally not stress-free, in agreement with other contributions (Latorre and Montáns, 2016; Ciambella et al.,*

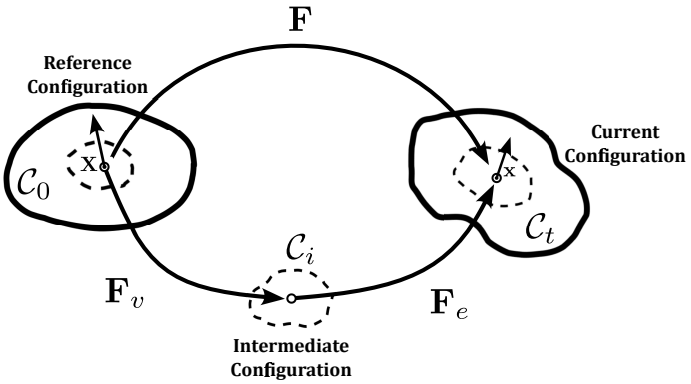


Figure 1: Representation of the introduced configurations.

*2024). When considering the multiplicative decomposition in Eq.* (7)*, it is worth noting that the system only reaches its thermodynamic equilibrium once the elastic deformation gradient* $\mathbf{F}_e$ *has finished evolving. This means that the relaxed intermediate configuration coincides then with the current configuration so that* $\mathbf{F} = \mathbf{F}_v$ *(see section 2 in Latorre and Montáns (2016)).*

Assuming that the volumetric part may show viscoelasticity and applying the multiplicative elastic/viscous decomposition, one gets,

$$\mathbf{F} = (J_e J_v)^{1/3}\, \bar{\mathbf{F}}_e\, \bar{\mathbf{F}}_v. \tag{8}$$

The following kinematic relations are then defined for the isochoric Cauchy-Green tensors related to the intermediate configuration,

$$\begin{cases} \bar{\mathbf{C}}_e = \bar{\mathbf{F}}_e^T\, \bar{\mathbf{F}}_e = \bar{\mathbf{F}}_v^{-T}\, \bar{\mathbf{C}}\, \bar{\mathbf{F}}_v^{-1}, & \text{(9a)} \\ \bar{\mathbf{b}}_v = \bar{\mathbf{F}}_v\, \bar{\mathbf{F}}_v^T = \bar{\mathbf{F}}_e^{-1}\, \bar{\mathbf{b}}\, \bar{\mathbf{F}}_e^{-T}. & \text{(9b)} \end{cases}$$

Furthermore, the spatial velocity gradient is then expressed in terms of its elastic part $\mathbf{l}_e = \dot{\mathbf{F}}_e\, \mathbf{F}_e^{-1}$ operating in the current configuration and its viscous part $\mathbf{l}_v = \dot{\mathbf{F}}_v\, \mathbf{F}_v^{-1}$ in the intermediate one,

$$\mathbf{l} = \mathbf{l}_e + \mathbf{F}_e\, \mathbf{l}_v\, \mathbf{F}_e^{-1}. \tag{10}$$

*2.3. Thermodynamic principles*

According to the theory of thermodynamic irreversible processes with internal variables (Coleman and Gurtin, 1967), independent sets of observable variables such

as temperature and strain tensors, as well as internal state variables such as viscoelastic strain tensors $\mathbf{A}_k$, are introduced. The Helmholtz free energy per unit mass $\psi$ is then introduced as a function of these thermodynamic variables. By assuming isothermal processes, the combination of thermodynamic conservation principles reduces to the Clausius-Duhem inequality,

$$\mathbf{S} : \frac{1}{2}\dot{\mathbf{C}} - \rho_0 \dot{\psi} \geq 0, \tag{11}$$

written here in a Lagrangian framework, introducing the mass density $\rho_0$ with respect to the reference configuration $\mathcal{C}_0$ and the second Piola-Kirchhoff stress tensor $\mathbf{S}$. Following the arguments of Coleman and Gurtin (1967), one gets the relation between the stress and the strain energy density $\mathcal{W}$,

$$\mathbf{S} = 2\rho_0 \frac{\partial \psi}{\partial \mathbf{C}} = 2\frac{\partial \mathcal{W}}{\partial \mathbf{C}}. \tag{12}$$

The remaining dissipation inequality enforces the following requirement for the internal variables $\mathbf{A}_k$,

$$-\sum_k \frac{\partial \mathcal{W}}{\partial \mathbf{A}_k} : \dot{\mathbf{A}}_k \geq 0, \tag{13}$$

which is classically satisfied for each $\mathbf{A}_k$ individually for simplicity purpose. In what follows, we will apply this assumption of internal variable separation since it has been adopted by the models that will be discussed.

Two approaches have been prevalent in the literature to ensure a consistent evolution of the internal variables. The two-potential framework (Germain et al., 1983) relies on the introduction of a dissipation potential $\Phi$, convex, positive and zero-valued at origin, function of the flow internal variables $\dot{\mathbf{A}}_k$ and such that,

$$\frac{\partial \mathcal{W}(\mathbf{A}_k)}{\partial \mathbf{A}_k} + \frac{\partial \Phi(\mathbf{A}_k, \dot{\mathbf{A}}_k)}{\partial \dot{\mathbf{A}}_k} = 0. \tag{14}$$

The dissipation potential $\Phi$ as well as the strain energy density $\mathcal{W}$ must satisfy the material symmetries, i.e. by remaining invariant under any change of reference configuration.

Provided that such a dissipation potential is defined, the thermodynamic consistency is automatically satisfied (Méo et al., 2002; Laiarinandrasana et al., 2003; Kumar and Lopez-Pamies, 2016). However, the existence of such a dissipation potential is not that simple a priori, and some authors have preferred to start from the internal dissipation inequality Eq. (13) to develop consistent evolution equations for their internal variables (Lion, 1997; Reese and Govindjee, 1998).

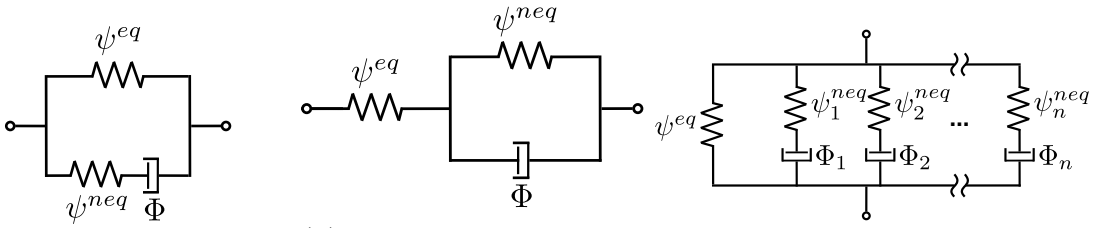


(a) Zener model (b) Poynting-Thompson model (c) generalized Maxwell model

Figure 2: Rheological schemes classically applied for the representation of viscoelastic materials.

### *2.4. Strain energy density $\mathcal{W}$*

By extension of the linear viscoelasticity to finite strain, rheological schemes defined by linear combinations of spring and dashpots in series or parallel are usually adopted. The Zener (Figure 2a) and Poynting-Thompson (Figure 2b) schemes are probably the most commonly used. Both tend towards the same equations in linear viscoelasticity but not in finite strain. As an extension of the Zener model, the generalized Maxwell scheme allows for several relaxation times through $n$ additional viscoelastic branches parallel to the purely elastic one (Figure 2c). Although not considered in this paper, developments about the Poynting-Thompson model may be found in (Huber and Tsakmakis, 2000; Boukamel et al., 2001; Méo et al., 2002; Laiarinandrasana et al., 2003).

Based on the Zener rheological scheme (Figure 2a), it is commonly assumed (Reese and Govindjee, 1998; Kumar and Lopez-Pamies, 2016) that the free energy $\psi$ may be additively decomposed into an equilibrium free energy $\psi^{eq}$ and non-equilibrium free energy $\psi^{neq}$. Accounting now for several relaxation mechanisms, one considers $n$ Maxwell branches ($k = 1, ..., n$) as in Figure 2c. Accordingly, the equilibrium part related to the purely elastic branch depends on the total deformation gradient $\mathbf{F}$, while the non-equilibrium parts related to the Maxwell branches depend on their corresponding elastic contribution $\mathbf{F}_e^k$ with $\mathbf{F} = \mathbf{F}_e^k \, \mathbf{F}_v^k$, so that,

$$\psi = \psi^{eq}(\mathbf{F}) + \sum_{k=1}^{n} \psi_k^{neq}(\mathbf{F}_e^k). \tag{15}$$

In passing, note the abuse of notation $\psi_k^{neq}(\mathbf{F}, \mathbf{F}_v^k) = \psi_k^{neq}(\mathbf{F}\,\mathbf{F}_v^{k\,-1}) = \psi_k^{neq}(\mathbf{F}_e^k)$ that is usually made (Latorre and Montáns, 2015; Kumar and Lopez-Pamies, 2016). In thermodynamic equilibrium, each free energy $\psi_k^{neq}$ is expected to vanish at a given

time, resulting in non-equilibrium stresses, also known as overstresses (Lion, 1997), equal to zero.

Following the volumetric-isochoric split of $\mathbf{F}$ in Eq. (6), the strain energy density may also be additively decomposed in the form,

$$\mathcal{W}(\mathbf{F}, \mathbf{F}_v^1, ..., \mathbf{F}_v^n) = \mathcal{U}(J, J_e^1, ..., J_e^n) + \overline{\mathcal{W}}(\bar{\mathbf{F}}, \bar{\mathbf{F}}_e^1, ..., \bar{\mathbf{F}}_e^n). \tag{16}$$

Due to material frame indifference, the strain energy density $\mathcal{W}$ reduces to a function of the right Cauchy-Green tensors,

$$\mathcal{W}(\mathbf{C}, \mathbf{C}_e^1, ..., \mathbf{C}_e^n) = \mathcal{U}(J, J_e^1, ..., J_e^n) + \overline{\mathcal{W}}(\bar{\mathbf{C}}, \bar{\mathbf{C}}_e^1, ..., \bar{\mathbf{C}}_e^n). \tag{17}$$

According to previous statements, both the volumetric and isochoric strain energy density functions $\mathcal{U}$ and $\overline{\mathcal{W}}$ can be split additively such as,

$$\begin{cases} \mathcal{U}(J, J_e^1, ..., J_e^n) = \mathcal{U}^{eq}(J) + \displaystyle\sum_{k=1}^{n} \mathcal{U}_k^{neq}(J_e^k), & \text{(18a)} \\ \overline{\mathcal{W}}(\bar{\mathbf{C}}, \bar{\mathbf{C}}_e^1, ..., \bar{\mathbf{C}}_e^n) = \overline{\mathcal{W}}^{eq}(\bar{\mathbf{C}}) + \displaystyle\sum_{k=1}^{n} \overline{\mathcal{W}}_k^{neq}(\bar{\mathbf{C}}_e^k). & \text{(18b)} \end{cases}$$

Furthermore, considering isotropic materials only, one may show that the strain energy density $\mathcal{W}$ writes as a function of the strain invariants,

$$\mathcal{W}(\mathbf{C}, \mathbf{C}_e^1, ..., \mathbf{C}_e^k) = \mathcal{U}^{eq}(J) + \sum_{k=1}^{n} \mathcal{U}_k^{neq}(J_e^k) + \overline{\mathcal{W}}^{eq}(\bar{I}_1, \bar{I}_2) + \sum_{k=1}^{n} \overline{\mathcal{W}}_k^{neq}(\bar{I}_{1e}^k, \bar{I}_{2e}^k), \tag{19}$$

where the classic notations have been introduced,

$$\begin{aligned} \bar{I}_1 &= \mathrm{tr}(\bar{\mathbf{C}}), \qquad \bar{I}_2 = \frac{1}{2}\left(\mathrm{tr}(\bar{\mathbf{C}})^2 - \mathrm{tr}(\bar{\mathbf{C}}^2)\right), \qquad J = \sqrt{\det(\mathbf{C})}, \\ \bar{I}_{1e}^k &= \mathrm{tr}\left(\bar{\mathbf{C}}_e^k\right), \quad \bar{I}_{2e}^k = \frac{1}{2}\left(\mathrm{tr}\left(\bar{\mathbf{C}}_e^k\right)^2 - \mathrm{tr}\left(\bar{\mathbf{C}}_e^{k\,2}\right)\right), \qquad J_e^k = \sqrt{\det\left(\mathbf{C}_e^k\right)}. \end{aligned} \tag{20}$$

The insertions of both volumetric and isochoric strain energy densities from Eq. (18) into the stress-strain relation Eq. (12) allow to define the material constitutive law, such as,

$$J\boldsymbol{\sigma} = \boldsymbol{\tau} = J\,\frac{\partial \mathcal{U}}{\partial J}\mathbf{I} + 2\,\mathrm{dev}\left(\bar{\mathbf{F}}\,\frac{\partial \overline{\mathcal{W}}^{eq}(\bar{\mathbf{C}})}{\partial \bar{\mathbf{C}}}\,\bar{\mathbf{F}}^T\right) + \sum_{k=1}^{n} 2\,\mathrm{dev}\left(\bar{\mathbf{F}}_e^k\,\frac{\partial \overline{\mathcal{W}}_k^{neq}(\bar{\mathbf{C}}_e^k)}{\partial \bar{\mathbf{C}}_e^k}\bar{\mathbf{F}}_e^{k\,T}\right). \tag{21}$$

To obtain the latter, the noteworthy relations between the stress tensors related to different configurations have been used,

$$J\boldsymbol{\sigma} = \boldsymbol{\tau} = \mathbf{P}\,\mathbf{F}^T = \mathbf{F}\,\mathbf{S}\,\mathbf{F}^T, \tag{22}$$

where $\boldsymbol{\sigma}$, $\boldsymbol{\tau}$ and $\mathbf{P}$ stand for the Cauchy, the Kirchhoff and the first Piola-Kirchhoff stress tensors, respectively.
Note that for isotropic materials, the strain energy density $\mathcal{W}$ may be equivalently written in terms of the left Cauchy-Green tensor $\mathbf{b}$ without loss of objectivity, as $\mathbf{b}$ and $\mathbf{C}$ tensors share the same invariants.

**Remark 4.** *It is worth mentioning that the general framework written as such leads to an indeterminacy on the intermediate configuration, which is known within a rotation. As it will appear in what follows, this indeterminacy does not need to be resolved in the case of isotropic materials.*

Models with viscoelastic strain internal variables that satisfy the thermodynamic requirement defined in Eq. (13) may differ in the choice of internal variables and associated evolution laws. The next section proposes a survey on the pioneering thermodynamically admissible finite strain viscoelastic models, comparing their internal variables and their associated evolution laws. For the sake of simplicity, constitutive equations are written for the Zener rheological scheme, given that the extension to the generalized Maxwell model is straightforward. In such a framework, note that the $k$ notation, used to distinguish several relaxation mechanisms, is dropped out from equations introduced previously to improve clarity. In addition, the viscosity parameters are assumed constant as further assessments about non-constant ones will be held in section 5.

## 3. Survey of finite strain viscoelastic models

The three pioneering finite strain viscoelastic models (Le Tallec et al., 1993; Lion, 1997; Reese and Govindjee, 1998) are first sorted according to the configuration of their internal variable definition. A rewriting with the same internal variable is then proposed in a second stage for comparison purposes.

### *3.1. Current configuration: Reese and Govindjee (1998) formulation*

Reese and Govindjee (1998) specified the non-equilibrium strain energy density $\mathcal{W}^{neq}$ as a function of $\mathbf{C}_e$, and wrote the Clausius-Duhem inequality (Eq. (13)) depending on spatial tensors,

$$-\frac{\partial \mathcal{W}^{neq}}{\partial \mathbf{C}_e} : \frac{\partial \mathbf{C}_e}{\partial \mathbf{F}_v} : \dot{\mathbf{F}}_v \geq 0 \quad \Longleftrightarrow \quad \frac{\partial \mathcal{W}^{neq}}{\partial \mathbf{C}_e} : (\mathbf{l}_v^T\,\mathbf{C}_e + \mathbf{C}_e\,\mathbf{l}_v) \geq 0\,, \tag{23}$$

which simply leads to,

$$2\frac{\partial \mathcal{W}^{neq}}{\partial \mathbf{C}_e} : (\mathbf{C}_e\, \mathbf{l}_v) \geq 0\,. \tag{24}$$

Then, by introducing the spatial elastic left Cauchy-Green tensor $\mathbf{b}_e = \mathbf{F}_e\, \mathbf{F}_e^T$ and the non-equilibrium Kirchhoff stress tensor $\boldsymbol{\tau}^{neq} = 2\,\mathbf{F}_e\, \frac{\partial \mathcal{W}^{neq}}{\partial \mathbf{C}_e}\, \mathbf{F}_e^T$, Eq. (24) may be rewritten in the form,

$$\boldsymbol{\tau}^{neq}\, \mathbf{b}_e^{-1} : \left(\mathbf{F}_e\, \mathbf{l}_v\, \mathbf{F}_e^T\right) \geq 0\,. \tag{25}$$

Even though the latter formulation is valid for anisotropic materials, it should be emphasized that the isotropy assumption makes $\boldsymbol{\tau}^{neq}$ and $\mathbf{b}_e$ commute, and thus $\boldsymbol{\tau}^{neq}\, \mathbf{b}_e^{-1}$ a symmetric tensor. Therefore, Eq. (25) reduces to,

$$-\boldsymbol{\tau}^{neq} : \frac{1}{2}(\mathcal{L}_v\, \mathbf{b}_e)\mathbf{b}_e^{-1} \geq 0\,, \tag{26}$$

where $\mathcal{L}_v \mathbf{b}_e$ stands for the Lie derivative of the contravariant tensor $\mathbf{b}_e$ and is defined as,

$$\mathcal{L}_v \mathbf{b}_e = \dot{\mathbf{b}}_e - \mathbf{l}\, \mathbf{b}_e - \mathbf{b}_e\, \mathbf{l}^T\,. \tag{27}$$

To satisfy Eq. (26), the authors finally proposed the following isotropic evolution (see Eq. (25) in (Reese and Govindjee, 1998)),

$$-(\mathcal{L}_v\, \mathbf{b}_e)\mathbf{b}_e^{-1} = \frac{1}{\eta_d}\mathrm{dev}(\boldsymbol{\tau}^{neq}) + \frac{2}{9\eta_h}\,(\boldsymbol{\tau}^{neq} : \mathbf{I})\,\mathbf{I}, \tag{28}$$

with distinct viscosity functions $\eta_h$ and $\eta_d$ for the hydrostatic and deviatoric parts. In addition, the authors assumed that $\eta_h$ and $\eta_d$ could be dependent on the elastic left Cauchy-Green tensor $\mathbf{b}_e$. As Kumar and Lopez-Pamies (2016) pointed out, such generality must be restricted to the tensor invariants to comply with the objectivity principle. Due to the fact that only constant viscosities are considered here, Eq. (28) may be finally rewritten (see Appendix B.1 for details) by splitting the volumetric and isochoric internal state variables, $J_v$ and $\bar{\mathbf{b}}_e$ respectively, into,

$$\begin{cases} \dot{J}_v = \dfrac{J}{\eta_h}\dfrac{\partial \mathcal{U}^{neq}(J_e)}{\partial J_e}\,, & \text{(29a)} \\ (\mathcal{L}_v\, \bar{\mathbf{b}}_e)\, \bar{\mathbf{b}}_e^{-1} = -\dfrac{1}{\eta_d}\,\mathrm{dev}\,(\boldsymbol{\tau}^{neq}) = -\dfrac{2}{\eta_d}\,\mathrm{dev}\left(\dfrac{\partial \overline{\mathcal{W}}^{neq}(\bar{\mathbf{b}}_e)}{\partial \bar{\mathbf{b}}_e}\,\bar{\mathbf{b}}_e\right). & \text{(29b)} \end{cases}$$

*3.2. Intermediate configuration: Lion (1997) formulation*

Lion (1997) addressed the finite strain viscoelastic equations in the intermediate configuration. In this framework, the strain tensor $\boldsymbol{\Gamma}$ defined with respect to the

intermediate configuration $\mathcal{C}_i$ is obtained by operating a push-forward of the Green-Lagrange tensor from the reference configuration $\mathcal{C}_0$ such as,

$$\mathbf{\Gamma} = \mathbf{F}_v^{-T}\,\mathbf{E}\,\mathbf{F}_v^{-1} = \frac{1}{2}\left(\mathbf{C}_e - \mathbf{I}\right) + \frac{1}{2}\left(\mathbf{I} - \mathbf{b}_v^{-1}\right) = \mathbf{\Gamma}_e + \mathbf{\Gamma}_v, \tag{30}$$

leading to the additive split of the strain tensor into its elastic and viscous parts. The stress tensor $\mathbf{T}^{neq}$ operating in $\mathcal{C}_i$ is obtained from the non-equilibrium second Piola-Kirchhoff stress tensor $\mathbf{S}^{neq}$ in a similar fashion,

$$\mathbf{T}^{neq} = \mathbf{F}_v\,\mathbf{S}^{neq}\,\mathbf{F}_v^{T} \quad \text{with} \quad \mathbf{S}^{neq} = \mathbf{S} - \mathbf{S}^{eq}. \tag{31}$$

In addition, the objective Oldroyd covariant derivative of the strain tensor $\mathbf{\Gamma}$ is defined as the push-forward of the rate of the Green-Lagrange tensor into the intermediate configuration, written as,

$$\overset{\triangle}{\mathbf{\Gamma}} = \mathbf{F}_v^{-T}\,\dot{\mathbf{E}}\,\mathbf{F}_v^{-1} = \dot{\mathbf{\Gamma}} + \mathbf{l}_v^{T}\,\mathbf{\Gamma} + \mathbf{\Gamma}\,\mathbf{l}_v. \tag{32}$$

By definition, this strain rate may also be additively split into elastic and viscous parts, such as,

$$\overset{\triangle}{\mathbf{\Gamma}} = \overset{\triangle}{\mathbf{\Gamma}}_e + \overset{\triangle}{\mathbf{\Gamma}}_v. \tag{33}$$

Interestingly, note that the last term simply equals to the viscous strain rate tensor, so that $\overset{\triangle}{\mathbf{\Gamma}}_v = \mathbf{d}_v = \frac{1}{2}\left(\mathbf{l}_v + \mathbf{l}_v^{T}\right)$. By introducing $\mathbf{\Gamma}_e$ into Eq. (13), and noticing that $\mathbf{S}^{neq} : \dot{\mathbf{E}} = \mathbf{T}^{neq} : \overset{\triangle}{\mathbf{\Gamma}}$, the Clausius-Duhem inequality from Eq. (11) thus becomes,

$$\left(\mathbf{T}^{neq} - \frac{\partial \mathcal{W}^{neq}}{\partial \mathbf{\Gamma}_e}\right) : \overset{\triangle}{\mathbf{\Gamma}}_e + \frac{\partial \mathcal{W}^{neq}}{\partial \mathbf{\Gamma}_e} : \overset{\triangle}{\mathbf{\Gamma}}_v + \frac{\partial \mathcal{W}^{neq}}{\partial \mathbf{\Gamma}_e} : \left(\mathbf{l}_v^{T}\,\mathbf{\Gamma}_e + \mathbf{\Gamma}_e\,\mathbf{l}_v\right) \geq 0. \tag{34}$$

Within the assumption of isotropy, the following simplification is then achieved,

$$\frac{\partial \mathcal{W}^{neq}}{\partial \mathbf{\Gamma}_e} : \left(\mathbf{l}_v^{T}\,\mathbf{\Gamma}_e + \mathbf{\Gamma}_e\,\mathbf{l}_v\right) = 2\mathbf{\Gamma}_e\,\frac{\partial \mathcal{W}^{neq}}{\partial \mathbf{\Gamma}_e} : \overset{\triangle}{\mathbf{\Gamma}}_v. \tag{35}$$

Accordingly, Lion proposed (see Eq. (31) in (Lion, 1997)) a sufficient condition to ensure a positive dissipation by specifying the simple evolution equation for the internal variable $\mathbf{\Gamma}_v$,

$$\overset{\triangle}{\mathbf{\Gamma}}_v = \frac{1}{\eta_v}\left(\mathbf{I} + 2\mathbf{\Gamma}_e\right)\frac{\partial \mathcal{W}^{neq}}{\partial \mathbf{\Gamma}_e} = \frac{1}{\eta_v}\mathbf{C}_e\mathbf{T}^{neq}. \tag{36}$$

Although the viscosity function $\eta_v$ is considered as constant here, Lion (1997) defined it as a function of the arguments $\mathbf{\Gamma}_v$ and $\mathbf{T}^{neq}$, and the temperature. Lastly, the author also accounted for volume changes by extending Eq. (36),

$$\begin{aligned}\overset{\triangle}{\bar{\mathbf{\Gamma}}}_v &= \frac{1}{\eta_v}\mathrm{dev}(\mathbf{C}_e\mathbf{T}^{neq}) + \frac{1}{3\eta_v}\left(\mathbf{C}_e\mathbf{T}^{neq} : \mathbf{I}\right)\mathbf{I} \\ &= \frac{1}{\eta_v}\mathrm{dev}\left(\bar{\mathbf{C}}_e\,\frac{\partial\overline{\mathcal{W}}^{neq}(\bar{\mathbf{\Gamma}}_e)}{\partial\bar{\mathbf{\Gamma}}_e}\right) + \frac{J_e}{\eta_v}\frac{\partial\mathcal{U}^{neq}}{\partial J_e}\mathbf{I}.\end{aligned} \tag{37}$$

Finally, further developments of Eq. (37), given in Appendix B.2, allow us to write the evolution equations of the internal variables in the intermediate configuration,

$$\begin{cases}\dot{J}_v = \dfrac{3J}{\eta_v}\dfrac{\partial\mathcal{U}^{neq}(J_e)}{\partial J_e}, & \text{(38a)}\\[2ex] \overset{\triangle}{\bar{\mathbf{\Gamma}}}_v = \dfrac{1}{\eta_v}\,\mathrm{dev}\left(\mathbf{F}_e^T\,\boldsymbol{\tau}^{neq}\,\mathbf{F}_e^{-T}\right) = \dfrac{1}{\eta_v}\,\mathrm{dev}\left(\left(\mathbf{I}+2\bar{\mathbf{\Gamma}}_e\right)\,\dfrac{\partial\overline{\mathcal{W}}^{neq}(\bar{\mathbf{\Gamma}}_e)}{\partial\bar{\mathbf{\Gamma}}_e}\right). & \text{(38b)}\end{cases}$$

Briefly, when comparing this volumetric evolution equation with Eq. (29a), one may note a difference with a factor of 3, while the isochoric one seems at first sight different from Eq. (29b). Finally, it is necessary to specify that the same viscosity functions are applied to hydrostatic and deviatoric parts, which means different relaxation times for both strain types. In contrast, Reese and Govindjee (1998) have chosen equal relaxation times, implying different bulk and shear viscosity functions in continuity with linear viscoelasticity.

### *3.3. Reference configuration: Le Tallec et al. (1993) formulation*

Prior to the former propositions, Le Tallec et al. (1993) have written finite strain viscoelastic constitutive equations for incompressible materials in a Lagrangian framework. The purpose here is to recall their constitutive equations and extend them to compressible materials to allow a comparison between all formulations.

First and foremost, Le Tallec et al. (1993) introduced the viscous right Cauchy-Green tensor $\mathbf{C}_v$ as their internal variable, which leads to write the internal dissipation inequality Eq. (13) as,

$$-\frac{\partial\mathcal{W}^{neq}}{\partial\mathbf{C}_v} : \dot{\mathbf{C}}_v \geq 0. \tag{39}$$

As the aforementioned models, the authors avoided the definition of a dissipation potential a priori. Hence, to ensure a positive dissipation rate, the most simple form is adopted for their internal variable,

$$-\nu\,\dot{\widehat{\mathbf{C}_v^{-1}}} = -\frac{\partial\mathcal{W}^{neq}}{\partial\mathbf{C}_v}, \tag{40}$$

where $\nu$ is a real-valued parameter associated with a viscosity. An important point to underline here is that Le Tallec et al. (1993) assumed $\mathbf{F}_v^{-1} = \sqrt{\mathbf{C}_v^{-1}}$, leading them to write $2\,\mathbf{d}_v = \sqrt{\mathbf{C}_v^{-1}}\,\dot{\mathbf{C}}_v\,\sqrt{\mathbf{C}_v^{-1}}$. It is then straightforward to show the positiveness of the internal dissipation Eq. (39) for all processes since

$$-\frac{\partial \mathcal{W}^{neq}}{\partial \mathbf{C}_v} : \dot{\mathbf{C}}_v = 4\,\nu\,\mathbf{d}_v : \mathbf{d}_v. \tag{41}$$

Additionally, the constitutive equations write for incompressible materials with isochoric viscoelastic processes in the form (see Eq. (3.10) in Le Tallec et al. (1993)),

$$\mathbf{S} = 2\frac{\partial \mathcal{W}}{\partial \mathbf{C}} - p\,\mathbf{C}^{-1} \qquad \text{and} \qquad -\nu\,\widehat{\dot{\mathbf{C}_v^{-1}}} = -\frac{\partial \mathcal{W}^{neq}}{\partial \mathbf{C}_v} + q\,\mathbf{C}_v^{-1} \tag{42}$$

with $p$ and $q$ unknown Lagrange multipliers. By considering then the simpler case of isotropic materials and using Eq. (B.24) from Appendix B.3, the former evolution equation turns into,

$$-\nu\,\widehat{\dot{\mathbf{C}_v^{-1}}} = \mathbf{F}_v^{-1}\,\frac{\partial \mathcal{W}^{neq}}{\partial \mathbf{C}_e}\,\mathbf{C}_e\,\mathbf{F}_v^{-T} + q\,\mathbf{C}_v^{-1}. \tag{43}$$

Lastly, by following the argument of incompressibility on both elastic and viscoelastic parts, one may show that

$$\frac{d}{dt}\left[\det(\mathbf{C}_v^{-1})\right] = \mathrm{tr}\left(\mathbf{C}_v\,\widehat{\dot{\mathbf{C}_v^{-1}}}\right) = 0 \quad \Longleftrightarrow \quad \mathrm{tr}\left(\frac{\partial \mathcal{W}^{neq}}{\partial \mathbf{C}_e}\,\mathbf{C}_e + q\,\mathbf{I}\right) = 0, \tag{44}$$

which provides the necessary expression of $q$ leading to the evolution equation of the internal variable $\mathbf{C}_v^{-1}$,

$$\widehat{\dot{\mathbf{C}_v^{-1}}} = -\frac{1}{\nu}\,\mathbf{F}_v^{-1}\,\mathrm{dev}\left(\frac{\partial \mathcal{W}^{neq}}{\partial \mathbf{C}_e}\,\mathbf{C}_e\right)\,\mathbf{F}_v^{-T}. \tag{45}$$

As a final step of this section, the development of the equation above in a compressible framework, detailed in Appendix B.3, leads to the following evolution equations,

$$\begin{cases} \dot{J}_v = \dfrac{J}{\eta_h}\dfrac{\partial \mathcal{U}^{neq}(J_e)}{\partial J_e}, & \text{(46a)} \\ \widehat{\dot{\bar{\mathbf{C}}_v^{-1}}} = -\dfrac{2}{\eta_d}\,\bar{\mathbf{F}}_v^{-1}\,\mathrm{dev}\left(\dfrac{\partial \overline{\mathcal{W}}^{neq}(\bar{\mathbf{C}}_e)}{\partial \bar{\mathbf{C}}_e}\,\bar{\mathbf{C}}_e\right)\,\bar{\mathbf{F}}_v^{-T}. & \text{(46b)} \end{cases}$$

Table 1: Summary of the constitutive equations of the three pioneering finite strain viscoelastic models as defined by their authors.

| **Model** | Reese and Govindjee (1998) | Lion (1997) | Le Tallec et al. (1993) |
|---|---|---|---|
| **Configuration** | *Current* | *Intermediate* | *Reference* |
| **Variable** | $\mathbf{b}_e$ | $\boldsymbol{\Gamma}_v$ | $\mathbf{C}_v^{-1}$ |
| **Objective Rate** | $\mathcal{L}_v\,\mathbf{b}_e$ (Lie) | $\overset{\triangle}{\boldsymbol{\Gamma}}_v$ (Oldroyd) | $\widehat{\dot{\mathbf{C}_v^{-1}}}$ |
| **Isochoric** | $-\frac{2}{\eta_d}\,\mathrm{dev}\left(\frac{\partial\overline{\mathcal{W}}^{neq}(\bar{\mathbf{b}}_e)}{\partial\bar{\mathbf{b}}_e}\,\bar{\mathbf{b}}_e\right)$ | $\frac{1}{\eta_v}\,\mathrm{dev}\left(\left(\mathbf{I}+2\bar{\boldsymbol{\Gamma}}_e\right)\,\frac{\partial\overline{\mathcal{W}}^{neq}(\bar{\boldsymbol{\Gamma}}_e)}{\partial\bar{\boldsymbol{\Gamma}}_e}\right)$ | $-\frac{2}{\eta_d}\,\bar{\mathbf{F}}_v^{-1}\,\mathrm{dev}\left(\frac{\partial\overline{\mathcal{W}}^{neq}(\bar{\mathbf{C}}_e)}{\partial\bar{\mathbf{C}}_e}\,\bar{\mathbf{C}}_e\right)\,\bar{\mathbf{F}}_v^{-T}$ |
| **Volumetric** | $\frac{J}{\eta_h}\frac{\partial\mathcal{U}^{neq}(J_e)}{\partial J_e}$ | $\frac{3J}{\eta_v}\frac{\partial\mathcal{U}^{neq}(J_e)}{\partial J_e}$ | $\frac{J}{\eta_h}\frac{\partial\mathcal{U}^{neq}(J_e)}{\partial J_e}$ |

*3.4. Comparison of evolution laws*

Considering the developments obtained from the three models above, the internal variables and evolution equations for both volumetric and isochoric parts are listed in Table 1. At first sight, only the volumetric evolution equations seem to be similar. Therefore, to compare the isochoric evolution laws in depth, the three models are rewritten in the reference configuration with the same internal variable, $\bar{\mathbf{C}}_v$.

For that purpose, the following noteworthy relationships are used

$$\mathcal{L}_v\,\bar{\mathbf{b}}_e = \bar{\mathbf{F}}\,\widehat{\dot{\overline{\mathbf{C}}_v^{-1}}}\,\bar{\mathbf{F}}^T\,,\quad \overset{\triangle}{\bar{\boldsymbol{\Gamma}}}_v = \frac{1}{2}\bar{\mathbf{F}}_v^{-T}\,\dot{\bar{\mathbf{C}}}_v\,\bar{\mathbf{F}}_v^{-1}\,,\quad \widehat{\dot{\overline{\mathbf{C}}_v^{-1}}} = -\bar{\mathbf{C}}_v^{-1}\,\dot{\bar{\mathbf{C}}}_v\,\bar{\mathbf{C}}_v^{-1}. \tag{47}$$

Note that the first and second equations are detailed in (Reese and Govindjee, 1998) and (Lion, 1997) respectively, while the last one is a simple definition. Recognizing also that,

$$\bar{\mathbf{F}}_e^{-1}\mathrm{dev}\left(\boldsymbol{\tau}^{neq}\right)\bar{\mathbf{F}}_e = 2\,\mathrm{dev}\left(\frac{\partial\overline{\mathcal{W}}^{neq}}{\partial\bar{\mathbf{C}}_e}\,\bar{\mathbf{C}}_e\right), \tag{48}$$

the rest comes straightforward from Eqs. (29b), (38b) and (46b) to,

$$\begin{cases} \text{Reese and Govindjee (1998)}: & \dot{\bar{\mathbf{C}}}_v = \frac{2}{\eta_d}\,\bar{\mathbf{F}}_v^T\,\mathrm{dev}\left(\frac{\partial\overline{\mathcal{W}}^{neq}}{\partial\bar{\mathbf{C}}_e}\,\bar{\mathbf{C}}_e\right)\,\bar{\mathbf{F}}_v, \\ \text{Lion (1997)}: & \dot{\bar{\mathbf{C}}}_v = \frac{4}{\eta_v}\,\bar{\mathbf{F}}_v^T\,\mathrm{dev}\left(\frac{\partial\overline{\mathcal{W}}^{neq}}{\partial\bar{\mathbf{C}}_e}\,\bar{\mathbf{C}}_e\right)\,\bar{\mathbf{F}}_v, \\ \text{Le Tallec et al. (1993)}: & \dot{\bar{\mathbf{C}}}_v = \frac{2}{\eta_d}\,\bar{\mathbf{F}}_v^T\,\mathrm{dev}\left(\frac{\partial\overline{\mathcal{W}}^{neq}}{\partial\bar{\mathbf{C}}_e}\,\bar{\mathbf{C}}_e\right)\,\bar{\mathbf{F}}_v. \end{cases} \tag{49}$$

An interesting outcome is that the indeterminate rotation part $\mathbf{R}_v$ that has been mentioned in Remark 4, drops out from the above equation with isotropic materials (Haupt, 2002). This becomes even more explicit when one rewrites the non-equilibrium strain energy density $\overline{\mathcal{W}}^{neq}$ as a function of elastic strain invariants,

$$\dot{\bar{\mathbf{C}}}_v = \frac{2}{\eta_d}\left[\bar{\alpha}\,\left(\bar{\mathbf{C}} - \frac{1}{3}\,\mathrm{tr}\left(\bar{\mathbf{C}}\,\bar{\mathbf{C}}_v^{-1}\right)\bar{\mathbf{C}}_v\right) + \bar{\beta}\,\left(\bar{\mathbf{C}}\,\bar{\mathbf{C}}_v^{-1}\,\bar{\mathbf{C}} - \frac{1}{3}\,\mathrm{tr}\left(\bar{\mathbf{C}}\,\bar{\mathbf{C}}_v^{-1}\,\bar{\mathbf{C}}\,\bar{\mathbf{C}}_v^{-1}\right)\bar{\mathbf{C}}_v\right)\right], \tag{50}$$

where the functions $\bar{\alpha} = \dfrac{\partial\overline{\mathcal{W}}^{neq}}{\partial\bar{I}_{1e}} + \bar{I}_{1e}\dfrac{\partial\overline{\mathcal{W}}^{neq}}{\partial\bar{I}_{2e}}$ and $\bar{\beta} = -\dfrac{\partial\overline{\mathcal{W}}^{neq}}{\partial\bar{I}_{2e}}$ have been introduced.

In addition, a careful reading of Eq. (49), clearly shows the difference by a factor of 2 between the evolution equation of Lion (1997) and the two others, this result being however consistent with Eq. (47.1) from (Lion, 1997). On this premise, the linearization of these models is in favor of (Le Tallec et al., 1993; Reese and Govindjee, 1998) for their solution, which recovers directly the classic infinitesimal strain equations. Finally, the major finding of this survey is that, even though the constitutive choices were quite different at the beginning, the three models finally define the same nonlinear evolution for their constitutive equations. One explanation for this result could stem from the simplest possible choice systematically made to ensure the positiveness of the dissipation, given that all models are based on the same underlying mechanical foundations, the thermodynamic principles and the Sidoroff (1974) multiplicative decomposition.

**Remark 5.** *Navigation between the different configurations, and thus between the different formulations, is made possible by means of the right push-forward / pull-back operations. A choice between one or the other formulation is then led by the problem at hand. Without getting into deep details about the resulting integration map arising from the choice of configuration, each exhibits pros and cons. First, the intermediate configuration has no physical meaning since a fictitious state was created by the multiplicative decomposition, so it is preferable to work with measurable*

*quantities. Second, the Lagrangian formulation is suitable for all kinds of materials, especially when dealing with anisotropic viscoelastic materials (Nguyen et al., 2007; Areias and Matouš, 2008; Latorre and Montáns, 2015; Reese et al., 2021), the calculations are made in the reference configuration and then push-forwarded to the current one to get the Cauchy stress. Third, the current configuration appears as a judicious selection to describe stress and strain, particularly for finite element implementation (Hasanpour et al., 2009), assuming that the proper tensors and objective rates are used.*

Finally, it is worth recalling that in previous studies, comparisons were made between two configurations: the reference and intermediate configuration (Lion, 1997; Naghdabadi et al., 2012), or the reference and current one (Latorre and Montáns, 2015). Lion (1997) specified the evolution equation in the reference configuration based only on strain invariants and did not discuss the connection between his formulation and that of Le Tallec et al. (1993). Naghdabadi et al. (2012) and Latorre and Montáns (2015) defined constitutive equations based on logarithmic strain tensors without providing a thorough comparison to former models. This point, among others, will be resolved in the next section.

### *3.5. Connection with other finite strain viscoelastic models*

Another model (Bergström and Boyce, 1998, 2001) played a major role in modeling the finite strain time-dependent behavior of incompressible rubberlike materials. Based on the physical representation of polymer chain extensions and reptations, they defined continuum mechanics constitutive equations that may be compared to the previous ones. Their theory starts with the additive decomposition of the spatial velocity tensor $\mathbf{l}$ as in Eq. (10),

$$\mathbf{l} = \mathbf{l}_e + \mathbf{F}_e\,\mathbf{l}_v\,\mathbf{F}_e^{-1} = \mathbf{l}_e + \overset{\sim}{\mathbf{l}}_v\,, \qquad \overset{\sim}{\mathbf{l}}_v = \overset{\sim}{\mathbf{d}}_v + \overset{\sim}{\mathbf{w}}_v. \tag{51}$$

The assumption of zero viscous spin rate, $\overset{\sim}{\mathbf{w}}_v = 0$, has been made by Bergström and Boyce (1998) in order to make the unloading unique (see also Bergström and Boyce (2001)). In addition, the Eulerian inelastic strain rate $\overset{\sim}{\mathbf{d}}_v$ is defined as a function of the deviatoric driving stress $\mathbf{N}$ and the effective creep rate function $\dot{\theta}$, this latter depending on both the inelastic stretch and stress invariants (see Eq. (13) and Eq. (24) in (Bergström and Boyce, 1998)). Thus, the evolution equation for this

model can be summarized as follows,

$$\begin{cases} \overset{\sim}{\mathbf{d}}_v = \dot{\theta}\,\mathbf{N}, \quad \mathbf{N} = \dfrac{\operatorname{dev}(\boldsymbol{\tau}^{neq})}{\tau_{iso}^{neq}}, & \text{(52a)} \\ \dot{\theta} = \dot{\theta}_0\,(\lambda_{chain}^{v} - 1 + \xi)^{C} \left(\dfrac{\tau_{iso}^{neq}}{\sqrt{2}\,\hat{\tau}}\right)^{m}, \quad \lambda_{chain}^{v} = \sqrt{\dfrac{tr(\mathbf{C}_v)}{3}}, & \text{(52b)} \end{cases}$$

with $\tau_{iso}^{neq} = ||\operatorname{dev}(\boldsymbol{\tau}^{neq})|| = \sqrt{\operatorname{dev}(\boldsymbol{\tau}^{neq}) : \operatorname{dev}(\boldsymbol{\tau}^{neq})}$ the effective stress measure, the reference creep rate $\dot{\theta}_0$, a dimension-purpose positive constant $\hat{\tau}$ and a material constant $C$ restricted to $[-1, 0]$ by reptational dynamic in the original contribution and later extended to $C < 0$ by (Dal and Kaliske, 2009). The parameter $\xi \to 0$, which was not present in the original version, has been introduced (Bergström and Boyce, 2001) to prevent numerical divergence when $\lambda_{chain}^{v} = 1$. As noted by other authors (Reese and Govindjee, 1998; Dal and Kaliske, 2009), this model replicates the model of Reese and Govindjee (1998) when a constant effective creep rate ($C = 0$, $m = 1$) is applied and the effective creep rate is expressed in terms of viscosity as $\dot{\theta} = \tau_{iso}^{neq}/(2\eta_d)$. In other words, the model of Bergström and Boyce (1998) can be seen as a variation of earlier models, with the key difference being that its viscosity depends on strain and stress levels. Additionally, this model has been implemented for finite element analyses, working either in a Lagrangian framework with Eq. (46b) (Areias and Matouš, 2008) or in an Eulerian framework with Eq. (29b) (Dal and Kaliske, 2009) following the implementation procedure proposed by Reese and Govindjee (1998).

Huber and Tsakmakis (2000) proposed finite strain viscoelastic laws for incompressible isotropic materials, modeled by either Zener or Poynting-Thompson rheological schemes, and defined in the intermediate configuration. The constitutive equations are the same as those proposed by Lion (1997), expressing the right part of Eq. (36) with a Mandel-like tensor instead. To model the high damping rubber behavior in shear and compression, Amin et al. (2002, 2006) reused the constitutive equations from Huber and Tsakmakis (2000). More specifically, they introduced a viscosity function depending on some invariants of $\mathbf{d}_v$ and Mandel-type stress tensor to represent well experimental features that, according to the authors, cannot be reproduced with constant viscosities.

Naghdabadi et al. (2012) proposed to introduce the logarithmic strain to express the evolution equation in a compressible framework. In doing so, both volumetric and isochoric equations were first written in an intermediate configuration (see Eq. (27)

in Naghdabadi et al. (2012)),

$$\widehat{\dot{\ln J_v}} = \frac{1}{\eta_h}\frac{\partial \mathcal{U}^{neq}}{\partial \ln J_e}, \qquad \bar{\mathbf{d}}_v = \frac{1}{\eta_d}\bar{\mathbf{F}}_e^T \frac{\partial \overline{\mathcal{W}}^{neq}}{\partial \bar{\mathbf{h}}_e}\bar{\mathbf{F}}_e^{-T} \quad \text{with} \quad \bar{\mathbf{h}}_e = \frac{1}{2}\ln \bar{\mathbf{b}}_e, \tag{53}$$

then restated into the initial configuration for the isochoric part (see Eq. (43) in Naghdabadi et al. (2012)),

$$\dot{\bar{\mathbf{C}}}_v = \frac{2}{\eta_d}\bar{\mathbf{U}}_v \frac{\partial \overline{\mathcal{W}}^{neq}}{\partial \bar{\mathcal{H}}_e}\bar{\mathbf{U}}_v \quad \text{with} \quad \bar{\mathcal{H}}_e = \frac{1}{2}\ln\left(\bar{\mathbf{U}}_v^{-1}\,\bar{\mathbf{C}}\,\bar{\mathbf{U}}_v^{-1}\right). \tag{54}$$

It is then straightforward to show that this hydrostatic evolution equation converges towards Eq. (29a). Moreover, Eq. (49) may be retrieved by applying some algebraic calculations on Eq. (54) (see (Sansour, 2001)). Latorre and Montáns (2015) have also chosen the Hencky logarithmic strain tensor to express the Clausius-Duhem inequality in both initial and current configurations, with an emphasis on anisotropic finite strain viscoelasticity. They offered an expression of the evolution of their internal variable in the reference configuration only. Interestingly, they have shown that their model recovers the one of Reese and Govindjee (1998) in the case of isotropy.

More recently, Kumar and Lopez-Pamies (2016) introduced a two-potential framework (as in Eq. (14)) to generalize the finite strain viscoelastic modeling of compressible materials. They highlighted the fact that finite models from Le Tallec et al. (1993), Reese and Govindjee (1998), and Bergström and Boyce (1998) are all part of their two-potential general framework, without clarifying their sameness as proposed here, but rather writing apparently different final expressions for the evolution laws.

Finally, it has been established that, when using a Zener rheological scheme with constant viscosity, the thermodynamically sound models discussed are essentially similar. Hence, we will refer to them as the *general model* and use Eq. (29) in what follows to ease the understanding. In passing, note that the formulation initially proposed by Le Tallec et al. (1993) may be seen as the incompressible limit of the *general model*.

In the next section, we propose to first compare the *general model* in uniaxial tension and simple shear to the still largely applied model of Simo (1987). To make the comparison as simple as possible, it should be emphasized that a simple Zener scheme is applied in section 4, implementing directly the evolution equations of the *general model* defined previously.

## 4. Comparison of the *general model* and Simo's model responses for simple loadings

This section aims at proposing a comparison between the *general model* and the model of Simo (1987) from a mere user perspective, due to the latter implementation in several finite element codes and its resulting prevalence when it comes to model viscoelasticity in finite strain. On that last point, it should be noted that the thermodynamic consistency of such models, based on hereditary integrals, is still an open debate. On the one hand, some contributions (Reese and Govindjee, 1997; Haslach, 2005; Govindjee et al., 2014; Latorre and Montáns, 2015) have pointed out that the thermodynamic requirements are not satisfied for all processes. On the other hand, Holzapfel and Simo (1996) claimed the thermodynamic consistency within some restrictive assumptions. Since the model of Simo (1987) is not our primary focus, interested readers may refer to (Govindjee et al., 2014; Liu et al., 2021) for further details about thermodynamic considerations and to (Drapaca et al., 2007; Ciambella et al., 2009; Wineman, 2009; De Pascalis et al., 2014; Berjamin et al., 2021; Yagimli et al., 2023) for theoretical developments and numerical implementations of some finite linear viscoelastic models.

### *4.1. Modeling inputs*

Briefly, the finite linear viscoelastic model of Simo (1987) may be summarized by the simple linear evolution equation,

$$\dot{\mathbf{Q}} + \frac{1}{\tau}\mathbf{Q} = \frac{d}{dt}\left[\mathrm{dev}\left(2\frac{\partial \overline{\mathcal{W}}^{neq}}{\partial \bar{\mathbf{C}}}\right)\right], \tag{55}$$

where $\mathbf{Q}$ is an internal variable of second Piola-Kirchhoff stress tensor type, usually distinct from $\bar{\mathbf{S}}^{neq}$ (see Liu et al. (2021) and references therein). Selecting $\mathbf{Q} = \bar{\mathbf{S}}^{neq}$ imposes restrictions in the constitutive equations to enforce the Clausius-Duhem inequality, as discussed in the preamble of this section.

Due to the linear form of Eq. (55), the internal variable may be estimated through the convolution integral,

$$\mathbf{Q} = \int_{-\infty}^{t} e^{-\frac{t-s}{\tau}} \frac{d}{ds}\left[\mathrm{dev}\left(2\frac{\partial \overline{\mathcal{W}}^{neq}}{\partial \bar{\mathbf{C}}}\right)\right] ds. \tag{56}$$

For the following, the model implemented in Abaqus (2021) was used to estimate the responses presented in the current contribution.

The comparisons are made for a Zener rheological representation, where only one relaxation time has been introduced. In addition, the simpler Neo-Hookean form is adopted for the isochoric part,

$$\overline{\mathcal{W}}(\bar{\mathbf{C}}, \bar{\mathbf{C}}_e) = \frac{\mu_\infty}{2}\left(\bar{I}_1(\bar{\mathbf{C}}) - 3\right) + \frac{\mu_e}{2}\left(\bar{I}_{1e}(\bar{\mathbf{C}}_e) - 3\right). \tag{57}$$

The following strain energy density was selected for the hydrostatic part,

$$\mathcal{U}(J, J_e) = \frac{K_\infty}{2} (J-1)^2 + \frac{K_e}{2} (J_e - 1)^2 . \tag{58}$$

For the numerical calculations, the elastic and viscoelastic shear moduli have been set to $\mu_\infty = 1$ MPa and $\mu_e/\mu_\infty = 9$. As for the elastic and viscoelastic bulk moduli, $K_\infty = K_e = 20\,\mu_\infty$, to exhibit some compressibility. It is worth noting that similar results have been obtained for bulk moduli at $10^3\,\mu_\infty$, with the only difference of displaying larger values for the stresses. Finally, the same relaxation time $\tau = 1$ s was applied for the hydrostatic and deviatoric parts and, by extension of the linearized theory, both viscosities are set to $\eta_h = K_e\,\tau$ and $\eta_d = \mu_e\,\tau$.

*4.2. Uniaxial tension*

For uniaxial tensile tests, the left Cauchy-Green tensor may be defined as,

$$\bar{\mathbf{b}} = \bar{\lambda}^2\,\vec{\mathbf{e}}_1 \otimes \vec{\mathbf{e}}_1 + \frac{1}{\bar{\lambda}} \left(\vec{\mathbf{e}}_2 \otimes \vec{\mathbf{e}}_2 + \vec{\mathbf{e}}_3 \otimes \vec{\mathbf{e}}_3\right), \tag{59}$$

where $\lambda$ stands for the stretch in the uniaxial loading direction.

Correspondingly, one may define the internal variable $\bar{\mathbf{b}}_e$ as the solution of the equation Eq. (29b) in the following form, by denoting $\bar{b}_j$ for $j \in \{1, 2, 3\}$ the components of $\bar{\mathbf{b}}_e$,

$$\bar{\mathbf{b}}_e = \bar{b}_1\,\vec{\mathbf{e}}_1 \otimes \vec{\mathbf{e}}_1 + \bar{b}_2\,\vec{\mathbf{e}}_2 \otimes \vec{\mathbf{e}}_2 + \bar{b}_3\,\vec{\mathbf{e}}_3 \otimes \vec{\mathbf{e}}_3, \tag{60}$$

with the isochoric constraint implying the relation $\bar{b}_2 = \bar{b}_3 = 1/\sqrt{\bar{b}_1}$. Finally, an analytical expression for the Cauchy stress is found by introducing both Eq. (57) and Eq. (58) into Eq. (12), and using the relationship Eq. (22),

$$\begin{aligned} \sigma_{11} = {} & K_\infty\,(J-1) + K_e \frac{J_e}{J}\,(J_e - 1) \\ & + \frac{2\mu_\infty}{3J} \left(\bar{\lambda}^2 - \frac{1}{\bar{\lambda}}\right) + \frac{2\mu_e}{3J} \left(\bar{\lambda}_e^2 - \frac{1}{\bar{\lambda}_e}\right), \end{aligned} \tag{61}$$

where non-equilibrium quantities $J_e = J/J_v$ and $\bar{b}_1 = \bar{\lambda}_e^2$ are estimated thanks to the dissipation equations Eqs. (29a) and (29b).

In Figure 3a, the stress-strain responses of both models are compared for monotonic uniaxial tensile loadings at several strain rates. Both models exhibit the same response for small stretches as they linearize into the infinitesimal strain model.

The models diverge at larger strains, indicating different linear vs. nonlinear evolution equations. As previously noted by Govindjee and Reese (1997), viscoelasticity dissipates more slowly in Simo's model than in the *general model*. This result

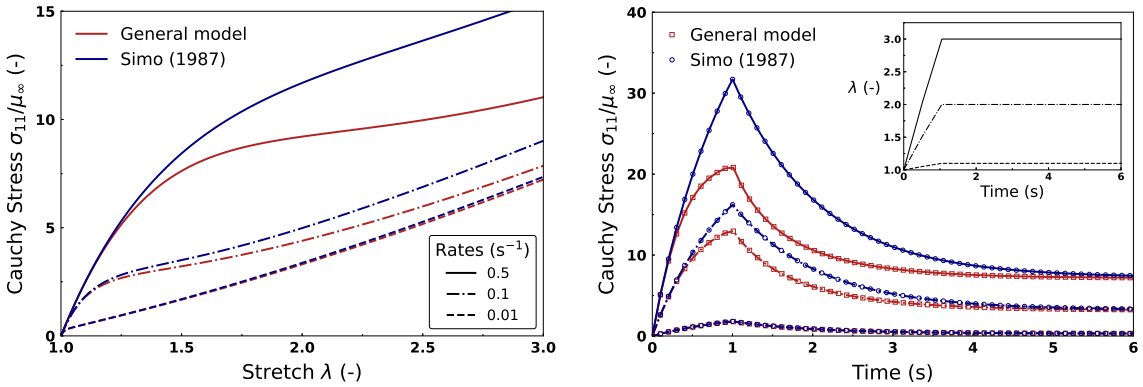


(a) (b)

Figure 3: Comparison of the *general model* and Simo's model stress-strain responses in uniaxial tension. (a) Monotonic uniaxial tensile loadings at several strain rates and (b) uniaxial tensile loadings at several strain rates followed by relaxation steps.

is also witnessed when applying relaxation steps. In Figure 3b, relaxations follow uniaxial tensile loadings performed at various strain rates during the same duration. As a result of these solicitations, one may note that the differences in the dissipative processes increase with the applied stretch.

### *4.3. Simple shear*

To model a simple shear loading, characterized by the amount of shear $\gamma$, the following deformation gradient tensor is adopted

$$\bar{\mathbf{F}} = \mathbf{I} + \gamma\, \vec{\mathbf{e}}_1 \otimes \vec{\mathbf{e}}_2. \tag{62}$$

The elastic tensor $\bar{\mathbf{b}}_e$ which results from such a loading writes as (Califano and Ciambella, 2023),

$$\bar{\mathbf{b}}_e = \bar{b}_1\, \vec{\mathbf{e}}_1 \otimes \vec{\mathbf{e}}_1 + \bar{b}_2\, \vec{\mathbf{e}}_2 \otimes \vec{\mathbf{e}}_2 + \bar{b}_3\, \vec{\mathbf{e}}_3 \otimes \vec{\mathbf{e}}_3 + \bar{b}_{12}\left(\vec{\mathbf{e}}_1 \otimes \vec{\mathbf{e}}_2 + \vec{\mathbf{e}}_2 \otimes \vec{\mathbf{e}}_1\right), \tag{63}$$

with the isochoric constraint implying $\bar{b}_3 = \left(\bar{b}_1\bar{b}_2 - \bar{b}_{12}^2\right)^{-1}$.

The corresponding Cauchy stress component $\sigma_{12}$ is written as,

$$\sigma_{12} = \tau_{12} = \mu_\infty\, \gamma + \mu_e\, \bar{b}_{12}, \tag{64}$$

where the component $\bar{b}_{12}$ may be evaluated using Eq. (29b).

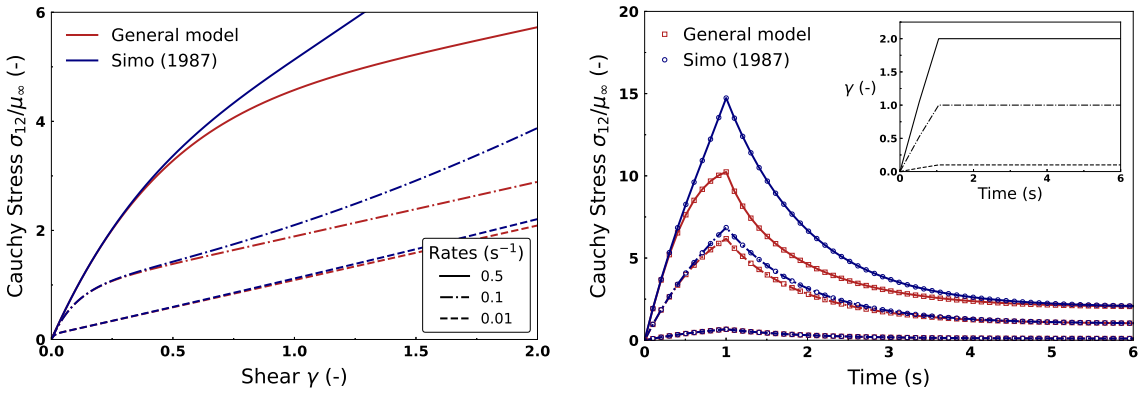


Figure 4: Comparison of the *general model* and Simo's model stress-strain responses in simple shear. (a) Monotonic shear loadings at several strain rates and (b) shear loadings at several strain rates followed by relaxation steps.

As shown in Figure 4, the same features are observed for simple shear loadings as in uniaxial tension. Additionally, as mentioned by (Califano and Ciambella, 2023) and illustrated in Figure 5, the Rivlin and Rideal (1948) relation, $\sigma_{11} - \sigma_{22} = \gamma\,\sigma_{12}$, always valid in hyperelasticity, may not hold in large viscoelastic deformations.

### *4.4. Sinusoidal loading*

Yagimli et al. (2023) recently conducted a study on the model's response of Simo (1987) to cyclic simple shear loadings with varying amplitudes. One significant finding is that noteworthy drawbacks are associated with the latter model. These include a non-physical overshooting behavior in a specific frequency range and a non-linear dependence of the stress response on shear amplitude, which is not expected for Neo-Hookean materials (see Figure 2 of the aforementioned paper). Such a significant dependence on amplitude has not yet been encountered with the *general model*. For instance, we have reproduced Yagimli et al. (2023) shear simulations and compared them to the *general model* in Figure 6. However, we have no general proof to offer since, unlike in (Yagimli et al., 2023) where an analytical solution has been obtained through the integration of linear equations, the integration of the nonlinear equations at hand (see Eq. (4.5) of Califano and Ciambella (2023)) is a much tedious task.

Yagimli et al. (2023) suggested improvements to the original constitutive equations of Simo (1987) to satisfactorily overcome the nonphysical overshooting. The same features as previously are observed when using the same parameters for the

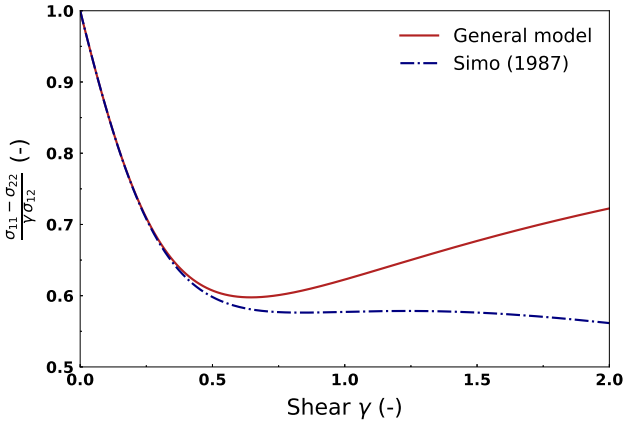


Figure 5: Rivlin and Rideal (1948) relation for monotonic simple shear at $0.1\,s^{-1}$ from Figure 4.

*general model* and the model of Yagimli et al. (2023). Precisely, the *general model* stands below at large strain amplitudes due to faster viscoelastic dissipation.

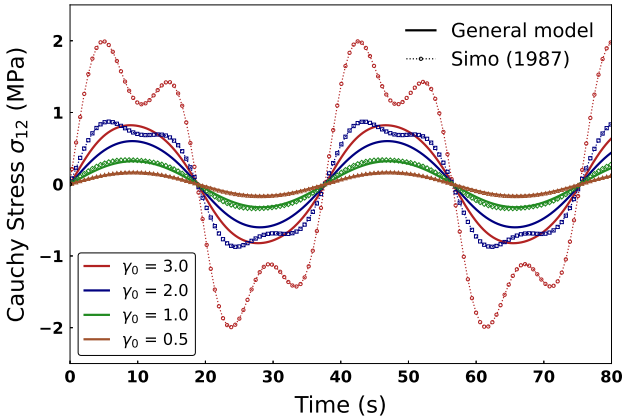


Figure 6: Comparison of the shear Cauchy stress $\sigma_{12}$ of the *general model* and Simo's model for various amplitudes at the angular frequency $\omega = \frac{1}{6}$ rad.s$^{-1}$ using a Zener scheme with material parameters $\mu_0 = \mu_\infty + \mu_e = 2$ MPa, $\mu_\infty = 2.0e^{-4}$ MPa and $\tau = 1$ s.

To further illustrate the nonlinear responses that may be obtained with the *general model*, Figure 7 shows the sinusoidal responses calculated for a shear amplitude of $\gamma_0 = 3$ and various angular frequencies. This is done when the Neo-Hookean strain energy density or the Gent (1996) model with $J_m = 9.1$ (using his notation) is chosen

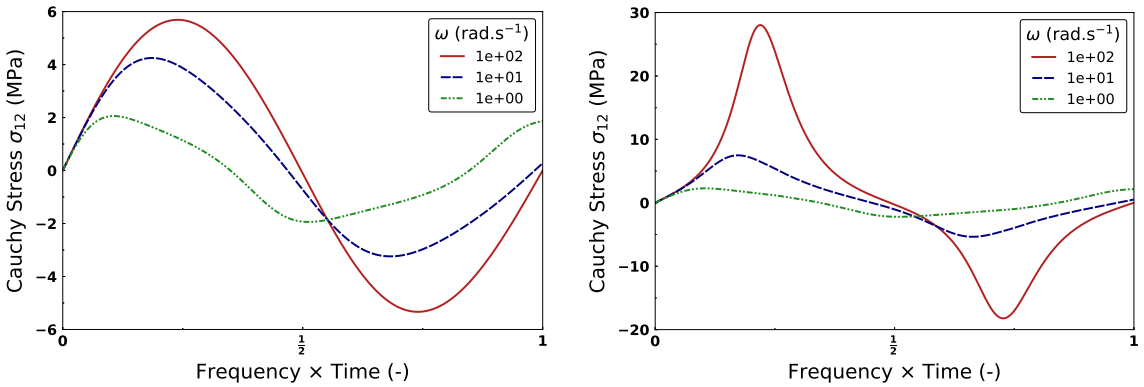


Figure 7: Shear Cauchy stress $\sigma_{12}$ at $\gamma_0 = 3$ of the *general model* for (a) Neo-Hookean and (b) Gent strain energy densities with different angular frequencies.

for $\overline{\mathcal{W}}$. As a result, the *general model* can exhibit significant nonlinearities depending on the loading frequency while avoiding unphysical behavior. The parameters used for Figure 6 are also applied here.

Considering now the *general model* only, two paths are generally followed, accounting for either constant viscosity parameters or non-constant ones. In the next section, we will closely examine the advantages and drawbacks of choosing a Zener model with non-constant viscosity or a generalized Maxwell model with constant viscosities.

## 5. Comparison of the generalized Maxwell model and the Zener model with non-constant viscosity

### *5.1. Zener model with a non-constant viscosity*

A discussion is proposed between two constitutive approaches defined to account for the multiple time-dependent behaviors of polymers, within the thermodynamically consistent framework exposed in section 3. The first one is based on the generalized Maxwell rheological scheme with $n$ viscoelastic branches that have constant parameters, by extension of infinitesimal strain viscoelasticity. The second one assumes a Zener rheological model with a non-constant viscosity function (Bergström and Boyce, 1998; Lion, 1997; Amin et al., 2006; Kumar and Lopez-Pamies, 2016). It may be challenging to accurately determine the parameters of the Prony series for

materials in the rubbery state, especially those far from the glass transition. Additionally, the computational cost of considering multiple Maxwell branches makes a compelling argument for using a simpler Zener model.

In the literature, various mathematical viscosity functions have been proposed (Ricker et al., 2023). Although these functions have different mathematical forms, they mostly share the same piloting variables, such as the non-equilibrium Kirchhoff stress invariant, $||\boldsymbol{\tau}^{neq}||$, or an inelastic strain invariant measure, typically $\bar{I}_{1v}$, or both. In this respect, Lion (1997) introduced a viscosity function that relies on variables defined in the intermediate configuration, making it difficult to measure or associate with a specific physical meaning. Dal et al. (2020) proposed a function that depends on the elastic strain invariant $\bar{I}_{1e}$, with however a similar form to the proposal from (Bergström and Boyce, 1998). Additionally, some authors proposed viscosities that are dependent on a scalar measure of the total strain, in addition to the inelastic strain (Miehe and Keck, 2000) or on the non-equilibrium Kirchhoff stress invariant (Haupt and Sedlan, 2001; Amin et al., 2006).

In a recent study, Ricker et al. (2023) tested the ability of several viscosity functions to replicate uniaxial tension cyclic tests with increasing maximum stretch, with and without relaxation steps. They found that the experimental data were better replicated using the three-parameter viscosity function (Eq. (52b)) from Bergström and Boyce (1998) and the six-parameter viscosity function from Kumar and Lopez-Pamies (2016),

$$\eta_d = \eta_\infty + \frac{\eta_0 - \eta_\infty + K_1(\bar{I}_{1v}^{\beta_1} - 3^{\beta_1})}{1 + (K_2\, J_2^{neq})^{\beta_2}}, \tag{65}$$

with invariants,

$$\begin{aligned} \bar{I}_{1v} &= \mathrm{tr}\left(\bar{\mathbf{b}}_v\right), \\ J_2^{neq} &= \frac{1}{2}||\mathrm{dev}\left(\boldsymbol{\tau}^{neq}\right)||^2 = \frac{1}{2}\mathrm{dev}\left(\boldsymbol{\tau}^{neq}\right) : \mathrm{dev}\left(\boldsymbol{\tau}^{neq}\right). \end{aligned} \tag{66}$$

The former refers to the viscous strain, while the latter is representative of the strain rate, since using Eqs. (48)-(49), one can show that $J_2^{neq} \propto \eta_d\, ||\dot{\bar{\mathbf{C}}}_v\, \bar{\mathbf{C}}_v^{-1}||$.

Focusing on the aforementioned models, with material parameters fitted by their authors on the same nitrile rubber experimental data (the parameters are listed in Tables 2 and 3), one may plot the viscosity changes according to $\bar{I}_{1v}$ and $J_2^{neq}$, by noticing that $\lambda_{chain}^v = \sqrt{\bar{I}_{1v}/3}$ and $\tau_v = \sqrt{J_2^{neq}}$ in Eq. (52b). Figure 8 shows both viscosities increasing similarly with the viscous strain invariant $\bar{I}_{1v}$. Additionally, both models show a reduction in viscosity as the strain rate $J_2^{neq}$ increases. However, only the six-parameter model (Kumar and Lopez-Pamies, 2016) exhibits plateaus that reproduce the shear thinning property of rubber materials.

| **Parameters** | **Values** | **Units** |
|---|---|---|
| $C_R^{(A)}$ | 0.29 | MPa |
| $C_R^{(B)}/C_R^{(A)}$ | 2.5 | - |
| $N^{(A)}$ | 6 | - |
| $N^{(B)}$ | 4 | - |
| $\hat{C} = \dot{\theta}_0/\hat{\tau}^m$ | 7 | $\mathrm{s}^{-1}.\mathrm{MPa}^{-m}$ |
| $C$ | $-0.6$ | - |
| $m$ | 5 | - |

Table 2: Parameters of the viscoelastic model from Bergström and Boyce (1998).

| **Parameters** | **Values** | **Units** |
|---|---|---|
| $\mu_1$ | 1.08 | MPa |
| $\mu_2$ | 0.017 | MPa |
| $\alpha_1$ | 0.26 | - |
| $\alpha_2$ | 7.68 | - |
| $m_1$ | 1.57 | MPa |
| $m_2$ | 0.59 | MPa |
| $a_1$ | $-10$ | - |
| $a_2$ | 7.53 | - |
| $\eta_\infty$ | 0.1 | MPa.s |
| $\eta_0$ | 2.11 | MPa.s |
| $K_1$ | 442 | MPa.s |
| $K_2$ | 1289.49 | $\mathrm{MPa}^{-2}$ |
| $\beta_1$ | 3 | - |
| $\beta_2$ | 1.929 | - |

Table 3: Parameters of the viscoelastic model from Kumar and Lopez-Pamies (2016).

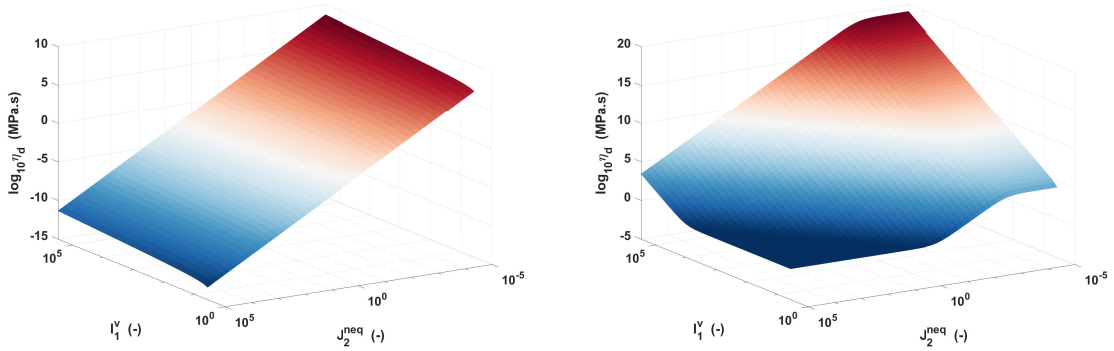


Figure 8: Changes with respect to $\bar{I}_{1v}$ and $J_2^{neq}$ of (a) Bergström and Boyce (1998) and (b) Kumar and Lopez-Pamies (2016) viscosity functions for parameters listed in Tables 2 and 3.

Now, for the comparison of Bergström and Boyce (1998) and Kumar and Lopez-Pamies (2016) models with a generalized Maxwell model, a simple method is proposed to identify the parameters of a Prony series that can satisfactorily represent the loading part of the stress-stretch response. Without having classic dynamic mechanical analysis tests in hand to determine the relaxation times and associated stiffnesses of the Prony series, sinusoidal tensile responses were generated numerically, setting the uniaxial stretch to,

$$\lambda(t) = \lambda_0 \sin(2\pi f\, t), \tag{67}$$

and estimating the stress response with the model of Kumar and Lopez-Pamies (2016). To remain in the linear regime, a small amplitude of $\lambda_0 = 0.001$ was considered, while the frequency $f$ was swept from $10^{-3}$ to $10^6$ Hz. The corresponding storage and loss Young moduli, $E'$ and $E''$, have been calculated using a Fast Fourier Transform analysis. Then, a viscoelastic spectrum $(E_k, \tau_k)$ from the Prony series is calculated based on the following formulae,

$$E'(\omega) = E_\infty + \sum_{k=1}^{n} E_k \frac{(\omega\,\tau_k)^2}{1+(\omega\,\tau_k)^2}, \quad E''(\omega) = \sum_{k=1}^{n} E_k \frac{\omega\,\tau_k}{1+(\omega\,\tau_k)^2}, \quad \tan\delta = E''/E'. \tag{68}$$

The results of this identification process, for an 8-branch Prony series with the simple Neo-Hookean model assuming incompressibility, are shown in Figure 9, with parameters listed in Table 4.

The comparison of the model performances is shown in Figure 10, displaying

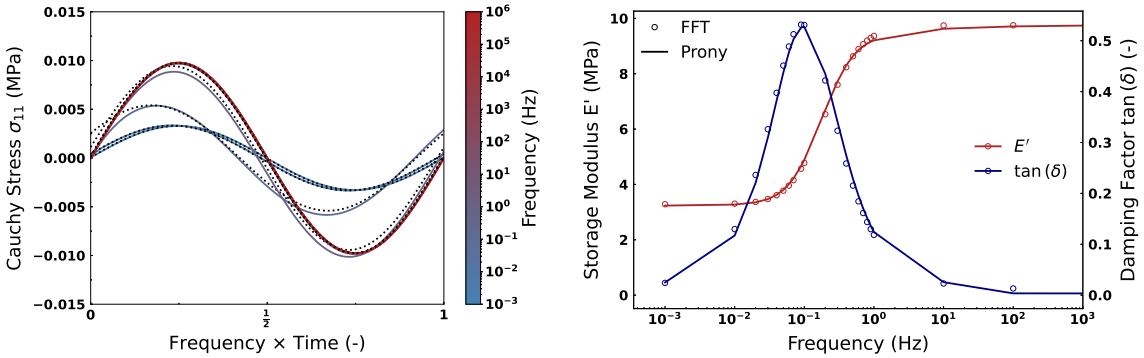


Figure 9: Prony series parameters identification: (left) Sinusoidal response for several frequencies generated with the model of Kumar and Lopez-Pamies (2016) and FFT analyses (dashed lines); (right) Corresponding storage modulus and damping factor.

the responses of the Prony series as well as both Zener models with non-constant viscosities, against Bergström and Boyce (1998) experimental data.

The generalized Maxwell model only provides satisfactory representations of the loading stress-stretch responses. Yet, the associated complex viscosity, defined by introducing the imaginary unit $i$ as,

$$\eta^* = \eta' - i\,\eta'' = \frac{G''}{\omega} - i\,\frac{G'}{\omega}\,, \tag{69}$$

shows a similar trend with respect to the frequency (Figure 11) to the one observed by Bergström and Boyce (1998) for $\eta_d$ vs. $J_2^{neq}$ (Figure 8). However, this similarity should be taken with care beyond the fact that $J_2^{neq}$ and $f$ are different quantities. Actually, the theoretical plots of $\eta_d$ shown in Figure 8 are not necessarily relevant since $\bar{I}_{1v}$ and $J_2^{neq}$ are coupled, and their coupling depends on the loading path. Consequently, it would be more compelling to observe how the viscosity changes during actual loading conditions. Next, we propose to estimate the stress-stretch responses of the Prony series and of Kumar and Lopez-Pamies (2016) model for several classic loading conditions with the previously listed parameters. Beyond comparing the stress-stretch responses, special attention will be paid to how the nonlinear viscosity behaves. Remarks about the viscosity function of Bergström and Boyce (1998) will be added when the trend differs from the one of Kumar and Lopez-Pamies (2016).

| **n** | $\tau_k$ **(s)** | $G_k$ **(MPa)** |
|---|---|---|
| $\infty$ | - | 0.79 |
| 1 | $2.35e^{-03}$ | 0.0438 |
| 2 | $9.98e^{-03}$ | 0.0855 |
| 3 | $2.81e^{-02}$ | 0.1666 |
| 4 | $7.01e^{-01}$ | 0.2921 |
| 5 | $1.20e^{+00}$ | 0.3226 |
| 6 | $1.11e^{+01}$ | 0.1522 |
| 7 | $1.00e^{+03}$ | 0.1824 |
| 8 | $3.93e^{+03}$ | 0.2125 |

Table 4: Parameters identified for a Neo-Hookean finite strain viscoelastic model with 8 Maxwell elements.

*5.2. Uniaxial loading/unloading*

It has been established that the generalized Maxwell model provides a poor representation of the hysteresis of the rubber data at hand. Especially, the model fails to reproduce the sharp drop of stress at the beginning of the unloading, unlike the model of Kumar and Lopez-Pamies (2016). To better understand the latter positive feature, we have plotted in Figure 12 the changes of viscosity during the loading/unloading uniaxial compression. At the beginning of unloading, the viscosity exhibits a sudden peak due to the rapid change in $J_2^{neq}$. This feature, which allows for a good reproduction of stress-strain responses, may be questionable from a physical standpoint. The experimental evidences reported, for instance, in (Bergström and Boyce, 1998; Bergström, 1999; Amin et al., 2006) show that at the peak stress of a loading-unloading cycle, filled rubbers exhibit stiffer behavior upon unloading than loading, even at very low applied strain rates. This raises questions about the significant change in viscosity required to replicate the experimental data. The physical and microstructural factors contributing to the stress drop at the start of unloading remain unclear as to whether it can be solely attributed to a change in viscosity.

*5.3. Relaxation at various strain amplitudes and strain rates*

It is noteworthy that when instantaneously stretching at various stretch levels $\lambda_0 = 1.1$, 1.5 or 2 and then applying a relaxation step, a model like Kumar and Lopez-Pamies (2016) may show stress relaxations that are dependent on the applied

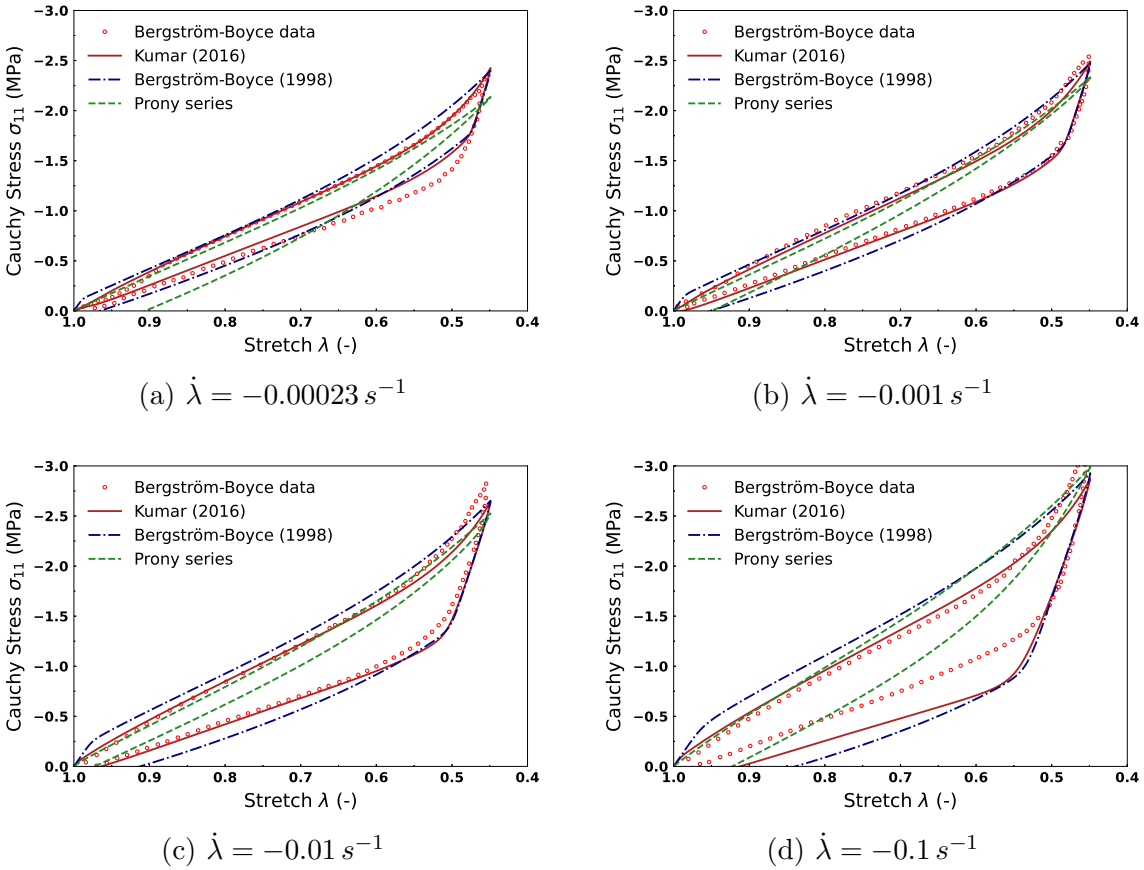


(a) $\dot{\lambda} = -0.00023\, s^{-1}$ (b) $\dot{\lambda} = -0.001\, s^{-1}$

(c) $\dot{\lambda} = -0.01\, s^{-1}$ (d) $\dot{\lambda} = -0.1\, s^{-1}$

Figure 10: Compression loading and unloading curves with viscosity functions of Kumar and Lopez-Pamies (2016) and Bergström and Boyce (1998) as well as the Prony series, in comparison with nitrile rubber data.

stretch, as illustrated in Figure 13. Such a behavior is due to the viscosity dependence on the stretch level and stretch rate. A generalized Maxwell model would show superimposed curves in place of Figure 13a. Depending on the chosen parameters, one may end up with a material that relaxes faster for larger stretches, as displayed here, or the opposite.

On the other hand, when considering uniaxial stretching up to $\lambda_0 = 1.5$ at several strain rates, the stress relaxations and the corresponding viscosity changes are depicted in Figure 14. During these relaxation processes, different slopes are observed depending on the initial strain rate value. In the 3D plot, the viscosity appears to follow the same path for all strain rates, suggesting a similar relationship based on

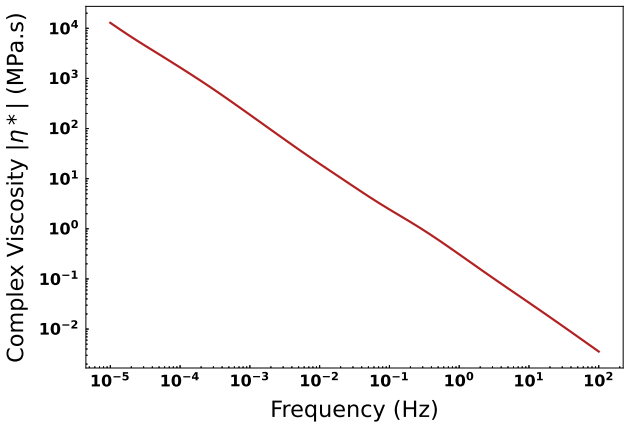


Figure 11: Evolution of the normalized complex viscosity $|\eta^*|$ according to the frequency for the identified Prony series.

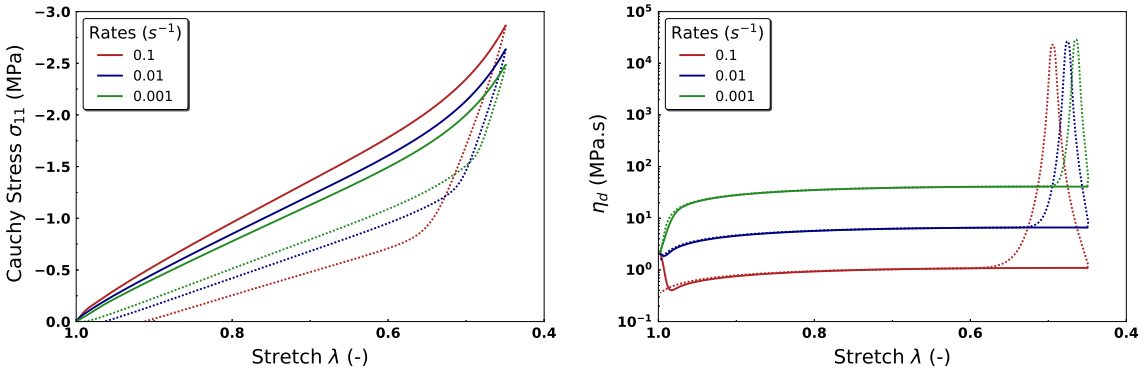


(a) (b)

Figure 12: Uniaxial tensile loading and unloading at various strain rates performed with the model of Kumar and Lopez-Pamies (2016): (a) Stress-stretch responses and (b) viscosity $\eta_d$ evolutions.

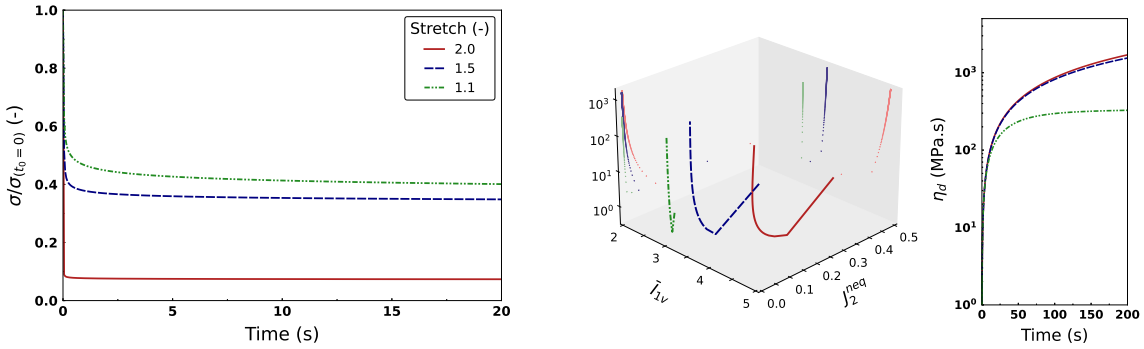


(a) (b)

Figure 13: Stress-stretch curves (a) and viscosity evolutions (b) for relaxations at different stretch levels reached instantaneously using the viscosity function of Kumar and Lopez-Pamies (2016).

both invariants. However, it is worth noting that the extreme value of $J_2^{neq}$ reached on this path varies depending on the initial strain rate. The generalized Maxwell model with constant parameters also provides the same general features, as shown in Figure 15. Therefore, both models may be considered as equivalent in such a case.

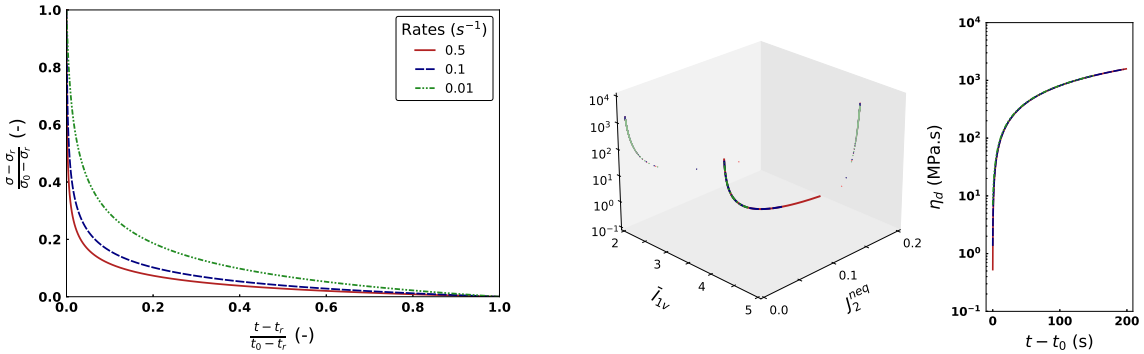


(a) (b)

Figure 14: Relaxation following monotonic uniaxial tensions at different strain rates until $\lambda_0 = 1.5$ for Kumar and Lopez-Pamies (2016) viscosity function. (a) Normalized stress-time curves and (b) viscosity evolution for the relaxation step.

### *5.4. Frequency dependence of the sinusoidal loading responses*

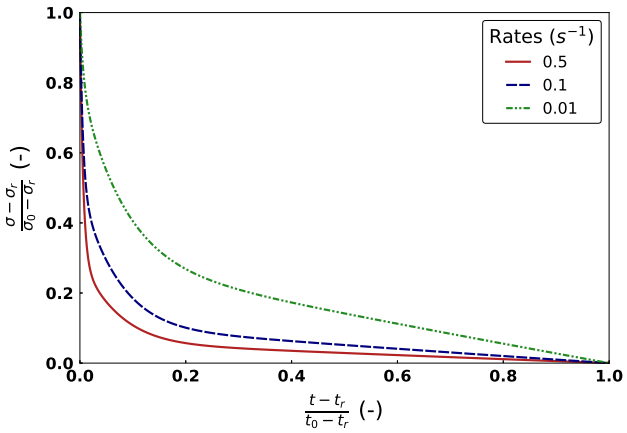


Figure 15: Stress relaxations following monotonic uniaxial tensions at different strain rates until $\lambda_0 = 1.5$ for the Prony series.

Similar to the sinusoidal shear loading in section 4.4, the stress vs. shear responses are shown in Figure 16a at various frequencies using the viscosity function of Kumar and Lopez-Pamies (2016). Unrealistic responses are witnessed within a specific range of frequencies, including 0.1 Hz, with the given parameters. This is illustrated by the butterfly-like shape of stress vs. shear plots. This undesired feature stems from the changes in the deviatoric stress invariant $J_2^{neq}$, which shows questionable peaks as illustrated in Figure 16b.

For comparative purposes, the same sinusoidal shear loadings are plotted in Figure 17a with the viscosity function from Bergström and Boyce (1998). At lower frequencies, the stress-shear plot shows rhomboid shapes leading to nonlinear sinusoidal responses even at small stretch amplitudes and low frequencies. To delve into this topic, examining the relationship between the viscosity function and the invariant $J_2^{neq}$ would be interesting, or introducing a more representative one. Finally, in contrast to the non-constant viscosity models, the identified Prony series exhibits classic hysteretic loops (Figure 17b).

## 6. Conclusions

A survey on the finite strain viscoelastic constitutive equations for rubberlike materials has been proposed. After introducing the classic mechanical framework for modeling finite viscoelasticity using a multiplicative decomposition of the deformation gradient tensor, the focus was placed on three pioneering models from the literature that unequivocally satisfy the thermodynamic requirements. By recall-

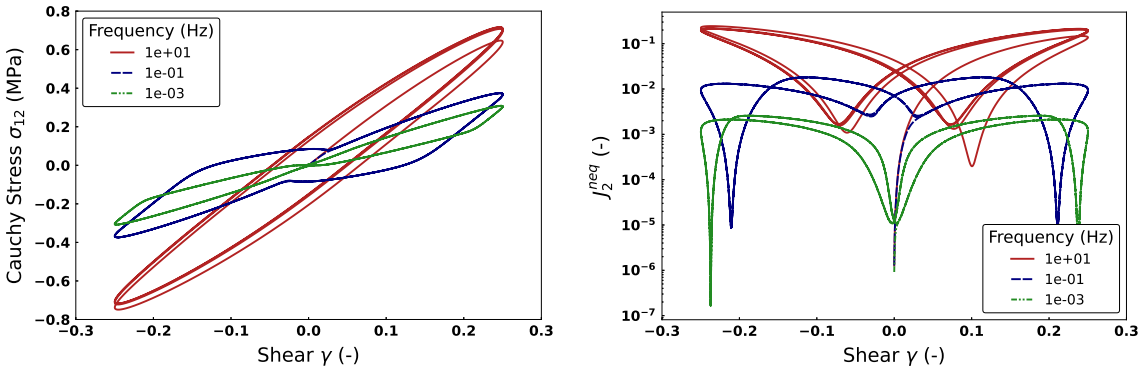


(a) (b)

Figure 16: Sinusoidal shear loadings at various frequencies and shear amplitude $\gamma_0 = 0.25$ with the viscosity function of Kumar and Lopez-Pamies (2016). (a) Stress vs. shear responses and (b) changes of $J_2^{neq}$ invariant.

ing the evolution equations defined in these papers and rewriting them in the same configuration, it has been possible to demonstrate that they merge into an identical *general model*. This result clarifies the state of the art and simplifies the path for future contributors to constitutive modeling of soft highly stretchable materials.

In the literature, authors have applied the *general model* to different rheological schemes, such as the generalized Maxwell one with constant viscosities and the Zener one with a non-constant nonlinear viscosity function. To better understand the interest of the latter option beyond its lower computational cost, both rheological schemes have been tested on various loading cases commonly used to characterize the mechanical behavior of rubberlike materials. It has been observed that, in general, more accurate data representations can be achieved through nonlinear viscosity functions. However, this improvement comes at the expense of questionable features such as sudden changes in viscosity during cyclic tests or viscosity fluctuations for sinusoidal loading, which lead to unsatisfactory concavity changes in the stress response. When the viscosity parameter is kept constant, it is possible to accurately reproduce the strain rate dependencies during loading and accurate stress relaxations by considering several Maxwell branches. However, it is impossible to replicate the sudden drop in stress at the beginning of the unloading part of cyclic tests and the dependence on the stretch amplitude, such as the Payne effect.

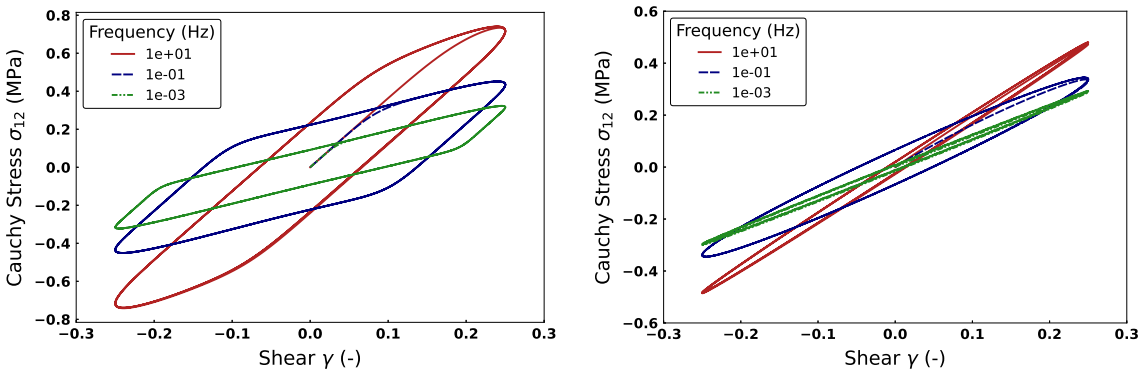


(a) (b)

Figure 17: Sinusoidal shear loading stress vs. shear responses at various frequencies and shear amplitude $\gamma_0 = 0.25$ for (a) the model of Bergström and Boyce (1998) and (b) the generalized Maxwell model.


## Acknowledgements

The authors gratefully acknowledge the financial support of ArianeGroup SAS, Centre de Recherches du Bouchet (France) and the Délégation Générale de l'Armement (DGA). Additionally, the authors thank Prof. P. Le Tallec for fruitful discussions.

## Appendix A. Nomenclature

Table A.5: Definitions and notations useful to the reader.

| Symbol | Calculation | Definition |
|---|---|---|
| | Mathematical operations and second-order tensor notations | |
| $\mathbf{I}$ | | Identity tensor |
| $\nabla$ | | Gradient operator |
| $\mathbf{X}^T$ | | Transpose of tensor $\mathbf{X}$ |
| $\mathbf{X}^{-1}$ | | Inverse of tensor $\mathbf{X}$ |
| $\mathbf{X} : \mathbf{Y}$ | $\mathrm{tr}(\mathbf{X}\,\mathbf{Y}^T)$ | Inner product of $\mathbf{X}$ and $\mathbf{Y}$ tensors |
| $\vec{\mathbf{x}} \otimes \vec{\mathbf{y}}$ | | Dyadic tensor-product of $\vec{\mathbf{x}}$ and $\vec{\mathbf{y}}$ vectors |
| $\|\|\mathbf{X}\|\|$ | $\sqrt{\mathbf{X} : \mathbf{X}}$ | Frobenius norm of $\mathbf{X}$ |
| $\mathrm{tr}(\mathbf{X})$ | | Trace of tensor $\mathbf{X}$ |
| $\mathrm{dev}(\mathbf{X})$ | $\mathbf{X} - \frac{1}{3}(\mathbf{X} : \mathbf{I})\,\mathbf{I}$ | Deviator operator in current configuration of $\mathbf{X}$ |
| $\det(\mathbf{X})$ | | Determinant of tensor $\mathbf{X}$ |
| $\mathrm{sym}(\mathbf{X})$ | $\frac{1}{2}\left(\mathbf{X} + \mathbf{X}^T\right)$ | Symmetric part of tensor $\mathbf{X}$ |
| $\mathrm{skew}(\mathbf{X})$ | $\frac{1}{2}\left(\mathbf{X} - \mathbf{X}^T\right)$ | Antisymmetric part of tensor $\mathbf{X}$ |
| $\bar{\mathbf{X}}$ | $\det(\mathbf{X})^{-1/3}\,\mathbf{X}$ | Isochoric part of tensor $\mathbf{X}$ |
| | Useful notations | |
| $\mathcal{C}_0$, $\mathcal{C}_i$, $\mathcal{C}_t$ | | Reference, intermediate and current configuration |
| $\dot{(\bullet)}$ | | Time derivative of quantity $(\bullet)$ |
| $(\bullet)_e,\ (\bullet)_v$ | | Elastic and viscous parts of quantity $(\bullet)$ |
| $(\bullet)^{eq},\ (\bullet)^{neq}$ | | Equilibrium and non-equilibrium parts of quantity $(\bullet)$ |
| $(\bullet)_d,\ (\bullet)_h$ | | Deviatoric and hydrostatic parts of quantity $(\bullet)$ |
| | Deformation variables | |
| $\mathbf{F}$ | | Deformation gradient tensor |
| $J$ | $\det(\mathbf{F})$ | Transformation Jacobian |
| $\mathbf{R}$ | $\mathbf{R}^{-1} = \mathbf{R}^T$ | Orthogonal rotation tensor |
| $\mathbf{U}$, $\mathbf{V}$ | | Right and left pure stretch tensors |

| | | |
|---|---|---|
| $\mathbf{C}$ | $\mathbf{F}^T\,\mathbf{F} = \mathbf{U}^2$ | Right Cauchy-Green stretch tensor |
| $\mathbf{b}$ | $\mathbf{F}\,\mathbf{F}^T = \mathbf{V}^2$ | Left Cauchy-Green stretch tensor |
| $\mathbf{E}$ | $\frac{1}{2}\,(\mathbf{C} - \mathbf{I})$ | Green-Lagrange strain tensor |
| $\mathbf{e}$ | $\frac{1}{2}\,(\mathbf{I} - \mathbf{b}^{-1})$ | Euler-Almansi strain tensor |
| $\mathbf{l}$ | $\dot{\mathbf{F}}\,\mathbf{F}^{-1}$ | Velocity gradient tensor |
| $\mathbf{d}$ | $\mathrm{sym}(\mathbf{l})$ | Deformation rate tensor |
| $\mathbf{w}$ | $\mathrm{skew}(\mathbf{l})$ | Spin tensor |
| $\mathcal{L}_v\mathbf{b}_e$ | $\dot{\mathbf{b}}_e - \mathbf{l}\,\mathbf{b}_e - \mathbf{b}_e\,\mathbf{l}^T$ | Lie derivative of the contravariant tensor $\mathbf{b}_e$ |
| $\boldsymbol{\Gamma}$ | $\mathbf{F}_v^{-T}\,\mathbf{E}\,\mathbf{F}_v^{-1}$ | Strain tensor related to $\mathcal{C}_i$ |
| $\overset{\triangle}{\boldsymbol{\Gamma}}$ | $\dot{\boldsymbol{\Gamma}} + \mathbf{l}_v^T\,\boldsymbol{\Gamma} + \boldsymbol{\Gamma}\,\mathbf{l}_v$ | Oldroyd derivative of the covariant tensor $\boldsymbol{\Gamma}$ |
| $\widetilde{\mathbf{l}}_v$ | $\mathbf{F}_e\,\mathbf{l}_v\,\mathbf{F}_e^{-1}$ | Viscous velocity gradient tensor related to $\mathcal{C}_t$ |
| $\widetilde{\mathbf{d}}_v,\ \widetilde{\mathbf{w}}_v$ | $\mathrm{sym}(\widetilde{\mathbf{l}}_v),\ \mathrm{skew}(\widetilde{\mathbf{l}}_v)$ | Viscous deformation rate and spin tensors related to $\mathcal{C}_t$ |
| | Energy | |
| $\psi$ | | Helmholtz free energy per unit mass |
| $\mathcal{W}$ | $\rho_0\psi$ | Strain energy density (per unit reference volume) |
| $\mathcal{U}$ | | Volumetric strain energy density |
| $\overline{\mathcal{W}}$ | | Isochoric strain energy density |
| $\Phi$ | | Dissipation potential |
| $p,\ q$ | | Lagrange multipliers |
| | Stress tensors | |
| $\mathbf{S}$ | $2\frac{\partial\mathcal{W}}{\partial\mathbf{C}}$ | Second Piola-Kirchhoff stress tensor |
| $\mathbf{P}$ | $\mathbf{F}\,\mathbf{S}$ | First Piola-Kirchhoff stress tensor |
| $\boldsymbol{\tau}$ | $\mathbf{F}\,\mathbf{S}\,\mathbf{F}^T$ | Kirchhoff stress tensor |
| $\boldsymbol{\sigma}$ | $\frac{1}{J}\mathbf{F}\,\mathbf{S}\,\mathbf{F}^T$ | Cauchy stress tensor |
| $\mathbf{T}^{neq}$ | $\mathbf{F}_v\,\mathbf{S}^{neq}\,\mathbf{F}_v^T$ | Non-equilibrium second Piola-Kirchhoff strain tensor in $\mathcal{C}_i$ |
| $\mathbf{Q}$ | | Internal variable of $\mathbf{S}$ type |

## Appendix B. Developments for the pioneering finite viscoelastic models

For what follows, let us remind two useful relations,

$$\frac{\partial(\mathrm{A}^{-1})_{ij}}{\partial(\mathrm{A})_{kl}} = -(\mathrm{A}^{-1})_{ik}\,(\mathrm{A}^{-1})_{lj}, \tag{B.1}$$

true for any second-order tensor $\mathbf{A}$, and

$$\frac{\partial J}{\partial \mathbf{C}} = \frac{J}{2}\mathbf{C}^{-1}, \tag{B.2}$$

when $J^2 = \det(\mathbf{C})$.

*Appendix B.1. Evolution equations of Reese and Govindjee (1998)*

This Appendix aims to provide the reader a deeper explanation about the transition from Eq. (28) to Eq. (29). First of all, the isotropic assumption allows to rewrite $\boldsymbol{\tau}^{neq}$ according to $\mathbf{b}_e$ as,

$$\boldsymbol{\tau}^{neq} = 2\mathbf{F}_e\frac{\partial \mathcal{W}^{neq}}{\partial \mathbf{C}_e}\mathbf{F}_e^T = 2\frac{\partial \mathcal{W}^{neq}}{\partial \mathbf{b}_e}\mathbf{b}_e. \tag{B.3}$$

Then, by definition, the non-equilibrium Kirchhoff stress tensor may be decomposed into deviatoric and hydrostatic parts and become,

$$\begin{aligned}\boldsymbol{\tau}^{neq} &= \mathrm{dev}\,(\boldsymbol{\tau}^{neq}) + \frac{1}{3}\,\mathrm{tr}\,(\boldsymbol{\tau}^{neq})\;\mathbf{I}\\ &= 2\frac{\partial \overline{\mathcal{W}}^{neq}}{\partial \mathbf{b}_e}\mathbf{b}_e + 2\frac{\partial \mathcal{U}^{neq}}{\partial \mathbf{b}_e}\mathbf{b}_e = 2\,\mathrm{dev}\left(\frac{\partial \overline{\mathcal{W}}^{neq}}{\partial \bar{\mathbf{b}}_e}\,\bar{\mathbf{b}}_e\right) + J_e\frac{\partial \mathcal{U}^{neq}}{\partial J_e}\,\mathbf{I}.\end{aligned} \tag{B.4}$$

Hence, the evolution equation proposed in Eq. (28) is rewritten in the form,

$$-(\mathcal{L}_v\,\mathbf{b}_e)\mathbf{b}_e^{-1} = \frac{2}{\eta_d}\,\mathrm{dev}\left(\frac{\partial \overline{\mathcal{W}}^{neq}}{\partial \bar{\mathbf{b}}_e}\,\bar{\mathbf{b}}_e\right) + \frac{2}{3\eta_h}J_e\,\frac{\partial \mathcal{U}^{neq}}{\partial J_e}\,\mathbf{I}, \tag{B.5}$$

and the split of $\mathbf{b}_e$ into isochoric and volumetric parts, as $\mathbf{b}_e = J_e^{2/3}\,\bar{\mathbf{b}}_e$, gives

$$(\mathcal{L}_v\,\mathbf{b}_e)\mathbf{b}_e^{-1} = (\mathcal{L}_v\,\bar{\mathbf{b}}_e)\bar{\mathbf{b}}_e^{-1} - \frac{2}{3}\frac{\dot{J}_v}{J_v}. \tag{B.6}$$

The evolution equations, as proposed in Eq. (29), are then obtained by equalizing deviatoric, respectively hydrostatic, parts from Eq. (B.5) with Eq. (B.6).

*Appendix B.2. Evolution equations of Lion (1997)*

Following the same procedure as before, the present Appendix aims to explain the transition from Eq. (37) to Eq. (38). For this purpose, the non-equilibrium stress tensor $\mathbf{C}_e\mathbf{T}^{neq} = \mathbf{C}_e\frac{\partial \mathcal{W}^{neq}}{\partial \mathbf{\Gamma}_e}$ may be decomposed into deviatoric and hydrostatic parts, such as,

$$\begin{aligned}\mathbf{C}_e\mathbf{T}^{neq} &= \mathrm{dev}\left(\mathbf{C}_e\mathbf{T}^{neq}\right) + \frac{1}{3}\,\mathrm{tr}\left(\mathbf{C}_e\mathbf{T}^{neq}\right)\,\mathbf{I} \\ &= \mathbf{C}_e\frac{\partial \overline{\mathcal{W}}^{neq}}{\partial \mathbf{\Gamma}_e} + \mathbf{C}_e\frac{\partial \mathcal{U}^{neq}}{\partial \mathbf{\Gamma}_e} = \mathrm{dev}\left(\bar{\mathbf{C}}_e\,\frac{\partial \overline{\mathcal{W}}^{neq}(\bar{\mathbf{\Gamma}}_e)}{\partial \bar{\mathbf{\Gamma}}_e}\right) + J_e\frac{\partial \mathcal{U}^{neq}}{\partial J_e}\,\mathbf{I}.\end{aligned} \tag{B.7}$$

Then, the evolution equation defined in Eq. (36) is now written as,

$$\overset{\triangle}{\mathbf{\Gamma}}_v = \frac{1}{\eta_v}\mathrm{dev}\left(\bar{\mathbf{C}}_e\,\frac{\partial \overline{\mathcal{W}}^{neq}(\bar{\mathbf{\Gamma}}_e)}{\partial \bar{\mathbf{\Gamma}}_e}\right) + \frac{J_e}{\eta_v}\frac{\partial \mathcal{U}^{neq}}{\partial J_e}\mathbf{I}, \tag{B.8}$$

and the split of the internal variable rate, $\overset{\triangle}{\mathbf{\Gamma}}_v = \mathbf{d}_v$, into isochoric and volumetric parts is given by applying the split $\mathbf{F}_v = J^{1/3}\bar{\mathbf{F}}_v$, such as

$$\mathbf{l}_v = \dot{\mathbf{F}}_v\mathbf{F}_v^{-1} = \bar{\mathbf{l}}_v + \frac{1}{3}\frac{\dot{J}_v}{J_v}\,\mathbf{I}, \quad \text{then} \quad \overset{\triangle}{\mathbf{\Gamma}}_v = \overset{\triangle}{\bar{\mathbf{\Gamma}}}_v + \frac{1}{3}\frac{\dot{J}_v}{J_v}\,\mathbf{I}. \tag{B.9}$$

The evolution equations, as proposed in Eq. (38), are then obtained by equalizing deviatoric, respectively hydrostatic, parts from Eq. (B.8) with Eq. (B.9).

*Appendix B.3. Evolution equations of Le Tallec et al. (1993)*

The current Appendix presents an extension to compressible materials of Le Tallec et al. (1993) formulation initially designed for isotropic incompressible ones.

First of all, we write the expressions of $\dfrac{\partial \bar{I}_{1e}}{\partial \bar{\mathbf{C}}_v}$ and $\dfrac{\partial \bar{I}_{2e}}{\partial \bar{\mathbf{C}}_v}$ that we will be needed. The first strain invariant $\bar{I}_{1e}$ is defined as,

$$\bar{I}_{1e} = \mathrm{tr}(\bar{\mathbf{C}}_e) = \bar{\mathbf{C}} : \bar{\mathbf{C}}_v^{-1}. \tag{B.10}$$

Then, by using the relationship Eq. (B.1),

$$\frac{\partial \bar{I}_{1e}}{\partial (\bar{\mathrm{C}}_v)_{kl}} = \frac{\partial (\bar{\mathrm{C}})_{ij}\,(\bar{\mathrm{C}}_v^{-1})_{ji}}{\partial (\bar{\mathrm{C}}_v)_{kl}} = -(\bar{\mathrm{F}}_v^{-1}\,\bar{\mathrm{C}}_e\,\bar{\mathrm{F}}_v^{-T})_{kl}\,, \tag{B.11}$$

$$\frac{\partial \bar{I}_{1e}}{\partial \bar{\mathbf{C}}_v} = -\,\bar{\mathbf{F}}_v^{-1}\,\bar{\mathbf{C}}_e\,\bar{\mathbf{F}}_v^{-T}. \tag{B.12}$$

By definition, the second invariant $\bar{I}_{2e}$ writes as,

$$\bar{I}_{2e} = \frac{1}{2}\left(\mathrm{tr}(\bar{\mathbf{C}}_e)^2 - \mathrm{tr}(\bar{\mathbf{C}}_e^2)\right) = \frac{1}{2}\left(\bar{I}_{1e}{}^2 - \mathrm{tr}(\bar{\mathbf{C}}_e^2)\right), \tag{B.13}$$

which gives,

$$\frac{\partial \bar{I}_{2e}}{\partial \bar{\mathbf{C}}_v} = \bar{I}_{1e}\,\frac{\partial \bar{I}_{1e}}{\partial \bar{\mathbf{C}}_v} - \frac{1}{2}\frac{\partial\,\mathrm{tr}(\bar{\mathbf{C}}_e^2)}{\partial \bar{\mathbf{C}}_v}. \tag{B.14}$$

By noting that,

$$\begin{aligned}\mathrm{tr}(\bar{\mathbf{C}}_e^2) &= \mathrm{tr}(\bar{\mathbf{F}}_v^{-T}\bar{\mathbf{C}}\bar{\mathbf{F}}_v^{-1}\,\bar{\mathbf{F}}_v^{-T}\bar{\mathbf{C}}\bar{\mathbf{F}}_v^{-1}) = \mathrm{tr}(\bar{\mathbf{F}}_v^{-1}\bar{\mathbf{F}}_v^{-T}\bar{\mathbf{C}}\,\bar{\mathbf{F}}_v^{-1}\bar{\mathbf{F}}_v^{-T}\bar{\mathbf{C}}) \\ &= \mathrm{tr}(\bar{\mathbf{C}}_v^{-1}\,\bar{\mathbf{C}}\;\bar{\mathbf{C}}_v^{-1}\,\bar{\mathbf{C}}),\end{aligned} \tag{B.15}$$

and using again Eq. (B.1), one finds,

$$\frac{\partial \mathrm{tr}(\bar{\mathbf{C}}_e^2)}{\partial(\bar{\mathrm{C}}_v)_{kl}} = -2(\bar{\mathrm{C}}_v^{-1}\,\bar{\mathrm{C}}\,\bar{\mathrm{C}}_v^{-1}\,\bar{\mathrm{C}}\,\bar{\mathrm{C}}_v^{-1})_{kl} = -2(\bar{\mathrm{F}}_v^{-1}\,\bar{\mathrm{C}}_e^2\,\bar{\mathrm{F}}_v^{-T})_{kl}\,. \tag{B.16}$$

Consequently, Eq. (B.14) writes as,

$$\frac{\partial \bar{I}_{2e}}{\partial \bar{\mathbf{C}}_v} = \bar{I}_{1e}\,\frac{\partial \bar{I}_{1e}}{\partial \bar{\mathbf{C}}_v} - \frac{1}{2}\frac{\partial\,\mathrm{tr}(\bar{\mathbf{C}}_e^2)}{\partial \bar{\mathbf{C}}_v} = -\bar{I}_{1e}\bar{\mathbf{F}}_v^{-1}\,\bar{\mathbf{C}}_e\,\bar{\mathbf{F}}_v^{-T} + \bar{\mathbf{F}}_v^{-1}\,\bar{\mathbf{C}}_e^2\,\bar{\mathbf{F}}_v^{-T}. \tag{B.17}$$

Following statements of Le Tallec et al. (1993), see Eq. (40), the evolution equation of $\mathbf{C}_v^{-1}$ may be written in a compressible case as,

$$-\nu\,\dot{\widehat{\mathbf{C}_v^{-1}}} = -\frac{\partial \mathcal{W}^{neq}}{\partial \mathbf{C}_v}. \tag{B.18}$$

The left part of this equation is now written thanks to the split of the internal variable $\dot{\widehat{\mathbf{C}_v^{-1}}}$ into its volumetric and isochoric parts, $J_v$ and $\bar{\mathbf{C}}_v^{-1} = J_v^{2/3}\mathbf{C}_v^{-1}$, introducing uncoupled viscosity functions,

$$-\nu\,\dot{\widehat{\mathbf{C}_v^{-1}}} = \nu_h\frac{2}{3}\frac{\dot{J}_v}{J_v^{5/3}}\bar{\mathbf{C}}_v^{-1} - \nu_d J_v^{-2/3}\dot{\widehat{\mathbf{C}_v^{-1}}}. \tag{B.19}$$

The right part of Eq. (B.18) becomes,

$$-\frac{\partial \mathcal{W}^{neq}(\bar{\mathbf{C}}_e, J_e)}{\partial \mathbf{C}_v} = -\left(\frac{\partial \mathcal{U}^{neq}(J_e)}{\partial \mathbf{C}_v} + \frac{\partial \overline{\mathcal{W}}^{neq}(\bar{I}_{1e}, \bar{I}_{2e})}{\partial \mathbf{C}_v}\right), \tag{B.20}$$

$$-\frac{\partial \mathcal{W}^{neq}(\bar{\mathbf{C}}_e, J_e)}{\partial \mathbf{C}_v} = \frac{J}{2J_v^{5/3}}\frac{\partial \mathcal{U}^{neq}(J_e)}{\partial J_e}\bar{\mathbf{C}}_v^{-1} - \frac{\partial \overline{\mathcal{W}}^{neq}(\bar{I}_{1e}, \bar{I}_{2e})}{\partial \mathbf{C}_v}, \tag{B.21}$$

when breaking down the non-equilibrium strain energy density function $\mathcal{W}^{neq}$ into pure volumetric $\mathcal{U}(J_e)$ and pure isochoric $\overline{\mathcal{W}}(\bar{\mathbf{C}}_e)$ parts.

Finally, comparing the volumetric parts of Eqs. (B.19) and (B.21), one gets,

$$\dot{J}_v = \frac{3J}{4\nu_h} \frac{\partial \mathcal{U}^{neq}(J_e)}{\partial J_e}. \tag{B.22}$$

As for the isochoric part of Eq. (B.21), $\dfrac{\partial \overline{\mathcal{W}}^{neq}}{\partial \mathbf{C}_v} = \dfrac{\partial \overline{\mathcal{W}}^{neq}}{\partial \bar{\mathrm{C}}_v} \dfrac{\partial \bar{\mathrm{C}}_v}{\partial \mathrm{C}_v}$, using the chain rule,

$$\frac{\partial \overline{\mathcal{W}}^{neq}}{\partial \bar{\mathbf{C}}_v} = \frac{\partial \overline{\mathcal{W}}^{neq}}{\partial \bar{I}_{1e}} \frac{\partial \bar{I}_{1e}}{\partial \bar{\mathbf{C}}_v} + \frac{\partial \overline{\mathcal{W}}^{neq}}{\partial \bar{I}_{2e}} \frac{\partial \bar{I}_{2e}}{\partial \bar{\mathbf{C}}_v}, \tag{B.23}$$

and the previous results Eqs. (B.12) and (B.17), one obtains

$$\frac{\partial \overline{\mathcal{W}}^{neq}}{\partial \bar{\mathbf{C}}_v} = -\bar{\mathbf{F}}_v^{-1} \frac{\partial \overline{\mathcal{W}}^{neq}}{\partial \bar{\mathbf{C}}_e} \bar{\mathbf{C}}_e \bar{\mathbf{F}}_v^{-T}, \tag{B.24}$$

and finally,

$$\begin{aligned} \frac{\partial \overline{\mathcal{W}}^{neq}}{\partial \mathbf{C}_v} &= \frac{\partial \overline{\mathcal{W}}^{neq}}{\partial \bar{\mathbf{C}}_v} \frac{\partial \bar{\mathbf{C}}_v}{\partial \mathbf{C}_v} = \frac{\partial \overline{\mathcal{W}}^{neq}}{\partial \bar{\mathbf{C}}_v} \frac{\partial (J_v^{-2/3} \mathbf{C}_v)}{\partial \mathbf{C}_v} \\ &= J_v^{-2/3} \left( \frac{\partial \overline{\mathcal{W}}^{neq}}{\partial \bar{\mathbf{C}}_v} - \frac{1}{3} \left( \frac{\partial \overline{\mathcal{W}}^{neq}}{\partial \bar{\mathbf{C}}_v} : \mathbf{C}_v \right) \mathbf{C}_v^{-1} \right). \end{aligned} \tag{B.25}$$

Hence, by comparing the isochoric parts of Eqs. (B.19) and (B.21), the isochoric internal variable rate is then defined as,

$$\overset{\cdot}{\widehat{\overline{\mathbf{C}}_v^{-1}}} = -\frac{1}{\nu_d} \bar{\mathbf{F}}_v^{-1} \operatorname{dev} \left( \frac{\partial \overline{\mathcal{W}}^{neq}}{\partial \bar{\mathbf{C}}_e} \bar{\mathbf{C}}_e \right) \bar{\mathbf{F}}_v^{-T}. \tag{B.26}$$

**Remark 6.** *The last two unknowns, $\nu_h$ and $\nu_d$, are then provided by comparison with the linear viscoelastic evolution equations written in a compressible framework in (Le Tallec et al., 1993),*

$$\begin{cases} \overset{\cdot}{\overline{tr\,\boldsymbol{\varepsilon}_v}} = \frac{3}{4} \frac{K_1}{\nu_h} \left( tr(\boldsymbol{\varepsilon}) - tr(\boldsymbol{\varepsilon}_v) \right) = \frac{1}{\tau} \left( tr(\boldsymbol{\varepsilon}) - tr(\boldsymbol{\varepsilon}_v) \right), \\ \dot{\boldsymbol{\varepsilon}}'_v = \frac{\mu_1}{2\nu_d} \left( \boldsymbol{\varepsilon}' - \boldsymbol{\varepsilon}'_v \right) = \frac{1}{\tau} \left( \boldsymbol{\varepsilon}' - \boldsymbol{\varepsilon}'_v \right), \end{cases} \tag{B.27}$$

*leading to the hydrostatic and deviatoric viscosity functions, $\nu_h = \frac{3}{4}\eta_h$ and $\nu_d = \frac{\eta_d}{2}$.*

## References


Abaqus, 2021. Standard. Dassault Systèmes Simulia Corp.

Amin, A.F.M.S., Alam, M.S., Okui, Y., 2002. An improved hyperelasticity relation in modeling viscoelasticity response of natural and high damping rubbers in compression: Experiments, parameter identification and numerical verification. Mechanics of Materials 34, 75–95.

Amin, A.F.M.S., Lion, A., Sekita, S., Okui, Y., 2006. Nonlinear dependence of viscosity in modeling the rate-dependent response of natural and high damping rubbers in compression and shear: Experimental identification and numerical verification. International Journal of Plasticity 22, 1610–1657.

Areias, P., Matouš, K., 2008. Finite element formulation for modeling nonlinear viscoelastic elastomers. Computer Methods in Applied Mechanics and Engineering 197, 4702–4717.

Bahreman, M., Darijani, H., Narooei, K., 2022. Investigation of multiplicative decompositions in the form of $F_eF_v$ and $F_vF_e$ to extend viscoelasticity laws from small to finite deformations. Mechanics of Materials 167, 104235.

Bergström, J.S., 1999. Large strain time-dependent behavior of elastomeric materials. Ph.D. thesis. Massachusetts Institute of Technology.

Bergström, J.S., Boyce, M.C., 1998. Constitutive modeling of the large strain time-dependent behavior of elastomers. Journal of the Mechanics and Physics of Solids 46, 931–954.

Bergström, J.S., Boyce, M.C., 2001. Constitutive modeling of the time-dependent and cyclic loading of elastomers and application to soft biological tissues. Mechanics of Materials 33, 523–530.

Berjamin, H., Destrade, M., Parnell, W.J., 2021. On the thermodynamic consistency of Quasi-linear viscoelastic models for soft solids. Mechanics Research Communications 111, 103648.

Bernstein, B., Kearsley, E.A., Zapas, L.J., 1963. A study of stress relaxation with finite strain. Transactions of The Society of Rheology 7, 391–410.

Boukamel, A., Méo, S., Débordes, O., Jaeger, M., 2001. A thermo-viscoelastic model for elastomeric behaviour and its numerical application. Archive of Applied Mechanics 71, 785–801.

Califano, F., Ciambella, J., 2023. Viscoplastic simple shear at finite strains. Proceedings of the Royal Society A: Mathematical, Physical and Engineering Sciences 479, 20230603.

Christensen, R.M., 1980. A nonlinear theory of viscoelasticity for application to elastomers. Journal of Applied Mechanics 47, 762–768.

Ciambella, J., Destrade, M., Ogden, R.W., 2009. On the ABAQUS FEA model of finite viscoelasticity. Rubber Chemistry and Technology 82, 184–193.

Ciambella, J., Lucci, G., Nardinocchi, P., 2024. Anisotropic evolution of viscous strain in soft biological materials. Mechanics of Materials 192, 104976.

Clifton, R.J., 1972. On the equivalence of $F^eF^p$ and $F^pF^e$. Journal of Applied Mechanics 39, 287–289.

Coleman, B.D., Gurtin, M.E., 1967. Thermodynamics with internal state variables. The Journal of Chemical Physics 47, 597–613.

Coleman, B.D., Noll, W., 1960. An approximation theorem for functionals, with applications in continuum mechanics. Archive for Rational Mechanics and Analysis 6, 355–370.

Coleman, B.D., Noll, W., 1961. Foundations of linear viscoelasticity. Rev. Mod. Phys. 33, 239–249.

Dal, H., Kaliske, M., 2009. Bergström–Boyce model for nonlinear finite rubber viscoelasticity: Theoretical aspects and algorithmic treatment for the FE method. Computational Mechanics 44, 809–823.

Dal, H., Osman, G., Kemal, A., 2020. An extended eight-chain model for hyperelastic and finite viscoelastic response of rubberlike materials: Theory, experiments and numerical aspects. Journal of the Mechanics and Physics of Solids 145, 104159.

De Pascalis, R., Abrahams, I.D., Parnell, W.J., 2014. On nonlinear viscoelastic deformations: A reappraisal of Fung's quasi-linear viscoelastic model. Proceedings of the Royal Society A: Mathematical, Physical and Engineering Sciences 470, 20140058.

Delattre, A., Lejeunes, S., Lacroix, F., Méo, S., 2016. On the dynamical behavior of filled rubbers at different temperatures: Experimental characterization and constitutive modeling. International Journal of Solids and Structures 90, 178–193.

Diani, J., Brieu, M., Vacherand, J.M., 2006. A damage directional constitutive model for Mullins effect with permanent set and induced anisotropy. European Journal of Mechanics - A/Solids 25, 483–496.

Drapaca, C.S., Sivaloganathan, S., Tenti, G., 2007. Nonlinear constitutive laws in viscoelasticity. Mathematics and Mechanics of Solids 12, 475–501.

Flory, P.J., 1961. Thermodynamic relations for high elastic materials. Trans. Faraday Soc. 57, 829–838.

Fung, Y.C., 1981. Biomechanics: Mechanical properties of living tissues. Springer-Verlag.

Gent, A.N., 1996. A New Constitutive Relation for Rubber. Rubber Chemistry and Technology 69, 59–61.

Germain, P., Nguyen, Q.S., Suquet, P., 1983. Continuum Thermodynamics. Journal of Applied Mechanics 50, 1010–1020.

Govindjee, S., Potter, T., Wilkening, J., 2014. Dynamic stability of spinning viscoelastic cylinders at finite deformation. International Journal of Solids and Structures 51, 3589–3603.

Govindjee, S., Reese, S., 1997. A presentation and comparison of two large deformation viscoelasticity models. Journal of Engineering Materials and Technology 119, 251–255.

Govindjee, S., Simo, J.C., 1992. Mullins' effect and the strain amplitude dependence of the storage modulus. International Journal of Solids and Structures 29, 1737–1751.

Green, A.E., Rivlin, R.S., 1959. The mechanics of non-linear materials with memory. Archive for Rational Mechanics and Analysis 4, 387–404.

Green, M.S., Tobolsky, A.V., 1946. A new approach to the theory of relaxing polymeric media. The Journal of Chemical Physics 14, 80–92.

Hasanpour, K., Ziaei-Rad, S., Mahzoon, M., 2009. A large deformation framework for compressible viscoelastic materials: Constitutive equations and finite element implementation. International Journal of Plasticity 25, 1154–1176.

Haslach, H.W., 2005. Nonlinear viscoelastic, thermodynamically consistent, models for biological soft tissue. Biomechanics and Modeling in Mechanobiology 3, 172–189.

Haupt, P., 2002. Continuum Mechanics and Theory of Materials. Springer Berlin Heidelberg. chapter Viscoelasticity. pp. 397–434.

Haupt, P., Sedlan, K., 2001. Viscoplasticity of elastomeric materials: Experimental facts and constitutive modelling. Archive of Applied Mechanics 71, 89–109.

Holzapfel, G.A., Gasser, T.C., Stadler, M., 2002. A structural model for the viscoelastic behavior of arterial walls: Continuum formulation and finite element analysis. European Journal of Mechanics - A/Solids 21, 441–463.

Holzapfel, G.A., Simo, J.C., 1996. A new viscoelastic constitutive model for continuous media at finite thermomechanical changes. International Journal of Solids and Structures 33, 3019–3034.

Huber, N., Tsakmakis, C., 2000. Finite deformation viscoelasticity laws. Mechanics of materials 32, 1–18.

Kaliske, M., Rothert, H., 1997. Formulation and implementation of three-dimensional viscoelasticity at small and finite strains. Computational Mechanics 19, 228–239.

Kumar, A., Lopez-Pamies, O., 2016. On the two-potential constitutive modeling of rubber viscoelastic materials. Comptes Rendus Mécanique 344, 102–112.

Kumar, N., Patel, B.P., Rao, V.V., Subhaschandran, B.S., 2018. Hyperviscoelastic constitutive modelling of solid propellants with damage and compressibility. Propellants, Explosives, Pyrotechnics 43, 461–471.

Laiarinandrasana, L., Piques, R., Robisson, A., 2003. Visco-hyperelastic model with internal state variable coupled with discontinuous damage concept under total Lagrangian formulation. International Journal of Plasticity 19, 977–1000.

Latorre, M., Montáns, F.J., 2015. Anisotropic finite strain viscoelasticity based on the Sidoroff multiplicative decomposition and logarithmic strains. Computational Mechanics 56, 503–531.

Latorre, M., Montáns, F.J., 2016. Fully anisotropic finite strain viscoelasticity based on a reverse multiplicative decomposition and logarithmic strains. Computers & Structures 163, 56–70.

Le Tallec, P., Rahier, C., Kaiss, A., 1993. Three-dimensional incompressible viscoelasticity in large strains: Formulation and numerical approximation. Computer Methods in Applied Mechanics and Engineering 109, 233–258.

Lee, E.H., 1969. Elastic-plastic deformation at finite strains. Journal of Applied Mechanics 36, 1–6.

Lion, A., 1997. A physically based method to represent the thermo-mechanical behaviour of elastomers. Acta Mechanica 123, 1–25.

Liu, J., Latorre, M., Marsden, A.L., 2021. A continuum and computational framework for viscoelastodynamics: I. Finite deformation linear models. Computer Methods in Applied Mechanics and Engineering 385, 114059.

Lockett, F., 1972. Nonlinear Viscoelastic Solids. Academic Press, London.

Lubarda, V.A., 1999. Duality in constitutive formulation of finite-strain elastoplasticity based on $F = F_e F_p$ and $F = F^p F^e$ decompositions. International Journal of Plasticity 15, 1277–1290.

Lubliner, J., 1985. A model of rubber viscoelasticity. Mechanics Research Communications 12, 93–99.

Mao, Y., Lin, S., Zhao, X., Anand, L., 2017. A large deformation viscoelastic model for double-network hydrogels. Journal of the Mechanics and Physics of Solids 100, 103–130.

Miehe, C., Keck, J., 2000. Superimposed finite elastic–viscoelastic–plastoelastic stress response with damage in filled rubbery polymers. Experiments, modelling and algorithmic implementation. Journal of the Mechanics and Physics of Solids 48, 323–365.

Mullins, L., 1969. Softening of rubber by deformation. Rubber Chemistry and Technology 42, 339–362.

Méo, S., Boukamel, A., Debordes, O., 2002. Analysis of a thermoviscoelastic model in large strain. Computers & Structures 80, 2085–2098.

Naghdabadi, R., Baghani, M., Arghavani, J., 2012. A viscoelastic constitutive model for compressible polymers based on logarithmic strain and its finite element implementation. Finite Elements in Analysis and Design 62, 18–27.

Nguyen, T.D., Jones, R.E., Boyce, B.L., 2007. Modeling the anisotropic finite-deformation viscoelastic behavior of soft fiber-reinforced composites. International Journal of Solids and Structures 44, 8366–8389.

Ogden, R.W., 1976. Volume changes associated with the deformation of rubber-like solids. Journal of the Mechanics and Physics of Solids 24, 323–338.

Özüpek, Ş., Becker, E.B., 1992. Constitutive modeling of high-elongation solid propellants. Journal of Engineering Materials and Technology 114, 111–115.

Payne, A., 1962. The dynamic properties of carbon black-loaded natural rubber vulcanizates. Part I. Journal of Applied Polymer Science 6, 57–63.

Pipkin, A.C., Rogers, T.G., 1968. A non-linear integral representation for viscoelastic behaviour. Journal of the Mechanics and Physics of Solids 16, 59–72.

Reese, S., Brepols, T., Fassin, M., Poggenpohl, L., Wulfinghoff, S., 2021. Using structural tensors for inelastic material modeling in the finite strain regime – A novel approach to anisotropic damage. Journal of the Mechanics and Physics of Solids 146, 104174.

Reese, S., Govindjee, S., 1997. Theoretical and numerical aspects in the thermo-viscoelastic material behaviour of rubber-like polymers. Mechanics of time-dependent materials 1, 357–396.

Reese, S., Govindjee, S., 1998. A theory of finite viscoelasticity and numerical aspects. International Journal of Solids and Structures 35, 3455–3482.

Rendek, M., Lion, A., 2010. Strain induced transient effects of filler reinforced elastomers with respect to the Payne-Effect: Experiments and constitutive modelling. ZAMM - Journal of Applied Mathematics and Mechanics 90, 436–458.

Ricker, A., Gierig, M., Wriggers, P., 2023. Multiplicative, non-newtonian viscoelasticity models for rubber materials and brain tissues: Numerical treatment and comparative studies. Archives of Computational Methods in Engineering 30, 2889–2927.

Rivlin, R.S., Rideal, E.K., 1948. Large elastic deformations of isotropic materials IV. Further developments of the general theory. Philosophical Transactions of the Royal Society of London. Series A, Mathematical and Physical Sciences 241, 379–397.

Sadik, S., Yavari, A., 2024. Nonlinear anisotropic viscoelasticity. Journal of the Mechanics and Physics of Solids 182, 105461.

Samadi-Dooki, A., Voyiadjis, G.Z., 2019. A fully nonlinear viscohyperelastic model for the brain tissue applicable to dynamic rates. Journal of Biomechanics 84, 211–217.

Sansour, C., 2001. On the dual variable of the logarithmic strain tensor, the dual variable of the Cauchy stress tensor, and related issues. International Journal of Solids and Structures 38, 9221–9232.

Schapery, R.A., 1964. Application of thermodynamics to thermomechanical, fracture, and birefringent phenomena in viscoelastic media. Journal of Applied Physics 35, 1451–1465.

Schapery, R.A., 1966. An engineering theory of nonlinear viscoelasticity with applications. International Journal of Solids and Structures 2, 407–425.

Sidoroff, F., 1974. Nonlinear viscoelastic model with an intermediate configuration. J. Mec. 13, 679–713.

Simo, J.C., 1987. On a fully three-dimensional finite-strain viscoelastic damage model: Formulation and computational aspects. Computer Methods in Applied Mechanics and Engineering 60, 153–173.

Simo, J.C., Ju, J.W., 1989. On continuum damage-elastoplasticity at finite strains. Computational Mechanics 5, 375–400.

Wang, C.C., 1965. Stress relaxation and the principle of fading memory. Archive for Rational Mechanics and Analysis 18, 117–126.

Wineman, A., 2009. Nonlinear viscoelastic solids—A review. Mathematics and Mechanics of Solids 14, 300–366.

Yagimli, B., Lion, A., Abdelmoniem, M.A., 2023. Analytical investigation of the finite viscoelastic model proposed by Simo: Critical review and a suggested modification. Continuum Mechanics and Thermodynamics 36, 369–390.

Yavari, A., Sozio, F., 2023. On the direct and reverse multiplicative decompositions of deformation gradient in nonlinear anisotropic anelasticity. Journal of the Mechanics and Physics of Solids 170, 105101.